

Identifying candidate hosts for quantum defects via data mining

Austin M. Ferrenti,[†] Nathalie P. de Leon,[‡] Jeff D. Thompson,[‡] and R. J. Cava[†]

[†] Department of Chemistry, Princeton University, Princeton, NJ 08544, USA

[‡] Department of Electrical Engineering, Princeton University, Princeton, NJ 08544, USA

Atom-like defects in solid-state hosts are promising candidates for the development of quantum information systems, but despite their importance, the host substrate/defect combinations currently under study have almost exclusively been found serendipitously. Here we systematically evaluate the suitability of host materials by applying a combined four-stage data mining and manual screening process to all entries in the Materials Project database, with literature-based experimental confirmation of band gap values. We identify 580 viable host substrates for quantum defect introduction and use in quantum information systems. While this constitutes a significant increase in the number of known and potentially viable material systems, it nonetheless represents a significant (99.54%) reduction from the total number of known inorganic phases, and the application of additional selection criteria for specific applications will reduce their number even further. The screening principles outlined may easily be applied to previously unrealized phases and other technologically important materials systems.

Introduction

In recent years, significant effort has been devoted to the realization of functional systems for quantum information science (QIS). QIS devices employ the manipulation of quantum states to store, process, and transmit information, potentially enabling the rapid solution of problems long thought impossible or impractical to address through classical methods. One of the most promising platforms for the development of efficient quantum information systems, particularly for application in quantum networks,¹ is atomic or atom-like defects in solid-state hosts.² The quantum coherence characteristics of the atomic defect, low defect concentrations, and quality of the host when combined should allow for long spin coherence and efficient optical transitions, properties also ideal for nanoscale sensing under ambient conditions.³

Several such atomic defect systems, including vacancy centers in diamond^{4–9} and silicon carbide¹⁰ have been extensively studied for several applications, in particular quantum networks,^{11,12} magnetometry and nanoscale sensors of magnetic fields,^{3,13,14} electric fields,¹⁵ temperature^{16,17} or chemical composition using NMR,^{18,19} often under ambient conditions at room temperature.²⁰ Another well-known class of defects is transition metal and rare earth ion impurities. These defects have been extensively explored in the context of solid-state laser development, in materials where extremely high doping concentrations are possible. However, exploring single defects as qubits is a more recent development,^{21,22} partially facilitated by integration with nano-photonic circuits to modify and enhance their luminescence.^{23,24} Although significant attention has thus far been paid to a handful of materials and defects, they represent only a small fraction of the greater body of potential defect-host systems. As most known quantum information materials systems have been discovered indirectly, a rational search of inorganic materials can yield candidates with superior properties.

Recent work has focused on *ab initio* predictions of host-defect systems that can be carried out with electronic structure calculations, as recently demonstrated with vacancy centers in silicon carbide,²⁵ and such calculations have been carried out for several individual host-defect combinations. An alternative approach is to systematically screen for potential host materials by first postulating which properties would be ideal for host material candidates, and then screen materials based on those properties. This is done most efficiently through a computational search that substantially narrows the field of potential candidates.

In order to achieve the long spin coherence and high efficiency optical transitions necessary for a usable quantum information system, host substrates must be highly pure (i.e. as free from defects as possible), intrinsically diamagnetic (thereby reducing magnetic noise and spin-based relaxation of the defect quantum state), and possess a band gap large enough to accommodate the ground and excited energy levels of the defect (separated by an optical frequency). The ideal, pure substrate would be free of paramagnetic impurities or unwanted defects that may influence the band gap character and/or a magnetic or electric field environment surrounding the implanted defect, reducing efficiency. Those materials known to be dopable, to possess controllable surfaces, and to possess a known method of epitaxial thin-film production would further facilitate the production of integrated devices.

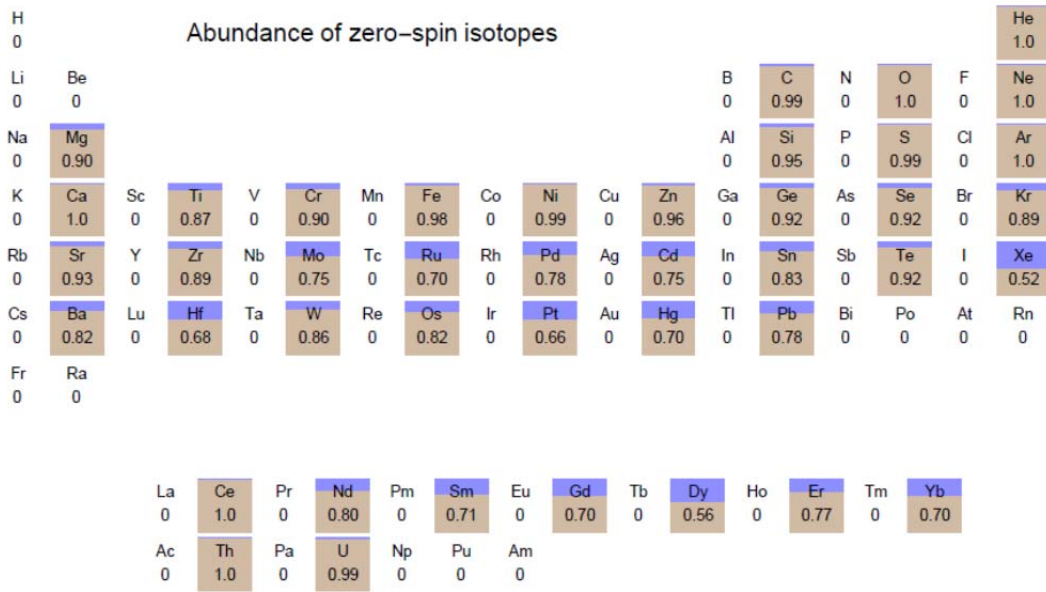


Figure 1. Color-coded periodic table depicting the natural abundance of stable zero nuclear spin isotopes, represented by the portion shaded gold ($I=0$) relative to the portion shaded blue ($I\neq 0$). Those elements for which there exist no stable spin-zero isotopes are shaded white.

Reducing magnetic noise and relaxation in the environment of the defect within the host requires both the minimization of paramagnetic centers in the host and the absence of host nuclei with non-zero magnetic moments. Consideration of the natural abundance of zero nuclear spin isotopes of each element, shown in Figure 1, allows for the exclusion of a significant portion of the periodic table, for which no stable spin-zero isotopes exist. While some elements, such as O and Ca, are known to exist almost exclusively as nuclear-spin-free isotopes, elemental species with at least 50% nuclear-spin-free isotopes could likely be isotopically enriched to higher

concentrations, as has been achieved in diamond^{26,27} and silicon²⁸. Although several of the lanthanide elements appear to have relatively high natural abundances of spin-free isotopes, the difficulty in obtaining pure, diamagnetic starting material of these (free from magnetic lanthanide impurities) excludes them from consideration here. All transition metal elements with unpaired electrons are eliminated due to their paramagnetism. As the optical coherence of defects may be sensitive to the presence of permanent electric dipole moments, and thus also to their site symmetry, phases crystallizing in polar space groups were also not considered.

In the current work, a systematic application of each of the criteria outlined above was performed, beginning with the totality of known inorganic phases listed in the Materials Project database. As the practice of database mining is often highly automated, the sensitivity of the desired properties to the exact phase and crystal structure reported for each potential host species necessitated manual checks after each restriction of the data set. While the true number of viable quantum host-defect pairings may be effectively infinite due to the fact that different quantum defects will be suitable for different applications, of the 100,000+ inorganic materials in the inorganic crystal structure database (ICSD), a maximum of 580 phases were found to be potentially viable hosts for atom-like defect quantum information systems. Among these, a small number are simple single elements or binary compounds, making them relatively straightforward to prepare and study as substrates for QIS.

Results and Discussion

To reduce the possibility of accidental exclusion of viable host materials, the screening of the Materials Project's 125,223 inorganic compound entries was conducted in four distinct stages, as shown in Figure 2.

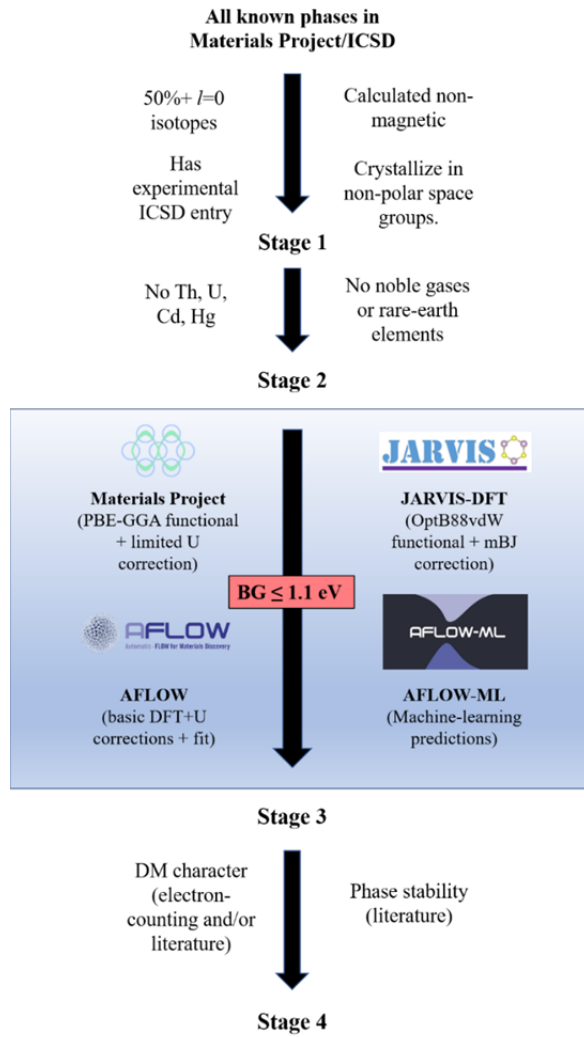


Figure 2. Four-tier screening process to evaluate the potential viability of materials as hosts for quantum defects. Stage 1) Beginning with all known experimental inorganic phases, remove those with calculated non-zero net magnetic moment, crystallization in polar space groups and/or containing atomic species with <50% $I=0$ isotopes. Stage 2) phases containing radioactive Th and U, toxic Cd and Hg, and the often magnetically impure rare earth elements were removed. The one phase containing a noble gas element that passed this sieve, orthorhombic XeO_3 , was also removed due to its known instability under standard conditions. Stage 3) The calculated, predicted, and measured experimental band gaps of the remaining phases were recorded from the Materials Project, the JARVIS-DFT database, the AFLOW repository, the AFLOW-ML API, and the existing literature. Those materials that could not be reasonably predicted to have a band gap larger than 1.1 eV were dismissed. Stage 4) The intrinsic diamagnetic (DM) character and phase stability under standard conditions of the remaining candidates were confirmed using a combination of standard electron-counting principles and literature reports. All database searches were conducted in February and March of 2020.

- 1) The first screen was applied utilizing the Materials Project's built-in query API²⁹, and removed all entries corresponding to phases crystallizing in polar space groups, derived from an experimental ICSD entry, containing only those elements with a greater than 50 percent natural abundance of zero nuclear spin isotopes, and calculated to be non-magnetic systems.
- 2) The second screen was applied by hand, and included the removal of all phases containing uranium, thorium, cadmium, and mercury, due to the radioactive and/or toxic nature of the majority of stable phases that each may form, as well as those containing noble gases, as none exist as stable solids under standard conditions. All rare-earth-element-containing phases were also removed, due to the difficulty in obtaining sufficiently pure starting materials free of nuclear spin.
- 3) The third and most important filter was applied utilizing calculated band gaps for all remaining phases reported by three publicly-available DFT computation repositories; the Materials Project, the Joint Automated Repository for Various Integrated Simulations (JARVIS), and the Automatic Flow of Materials Discovery (AFLOW) library, each of which employs a different band gap calculation and/or prediction method. In addition, where available, the Machine Learning-predicted band gap reported by Isayev *et al* in their predictive modeling studies was also taken into consideration.

At this stage, those phases with a Materials Project band gap of 2.0 eV were deemed likely to possess a large enough band gap to accommodate the necessary optical transitions of useful quantum defects, and, so as not to miss any potentially viable candidates, only those with calculated band gaps <0.5 eV were removed. For all other phases, any reports of experimental or otherwise calculated band gaps in the literature were taken into consideration. Various higher-order compounds for which the calculated band gaps were insufficient, such as in the Ba-Hf-S family, were approved based on general band gap trends. Those phases with calculated and/or experimentally-derived band gaps consistently in the range of that of Si, which would represent the lower bound of viability for potential host materials, are grayed in Tables 1-4.

The Materials Project³⁰ utilizes the DFT-based Vienna ab initio simulation package (VASP) software³¹ to calculate a wide variety of structural, energetic, and electronic properties for all reported inorganic structures in the Inorganic Crystal Structure Database (ICSD). An initial relaxation of cell and lattice parameters is performed using a 1,000 k -point mesh to ensure that all properties calculated are representative of the idealized unit cell for each material in its

respective crystal structure. To calculate band structures for these materials, the Generalized Gradient Approximation (GGA) functional is applied to the relaxed structures. For structures containing one of several transition metal elements such as Cr, Fe, Mo, and W, the +U correction is also applied to correct for correlation effects in occupied d- and f-orbital systems that are not addressed by pure GGA calculations.³² The authors caution that due to the high computational cost of more sophisticated calculation methods, those employed often produce severely underestimated band gaps relative to the experimentally-derived values.

JARVIS-DFT³³, originally compiled as a database for functional materials, with a focus on the discovery of novel two-dimensional systems, also employs the DFT-based VASP software to perform a variety of material property calculations. As opposed to the Materials Project, JARVIS-DFT employs the OptB88vdW (OPT) functional, which was initially designed to better approximate the properties of two-dimensional van der Waals materials, and has since also been shown to be effective for bulk systems.^{34,35} Structures are first sourced from the Materials Project database, and then re-optimized using the OPT functional. A representative band gap is then calculated through a combination of the OPT and modified Becke-Johnson (mBJ) functionals. The mBJ and combined OPT-mBJ functionals have both been shown to predict band gap sizes with more accuracy than other DFT-based calculation methods.³⁶

The **AFLOW**³⁷ repository relies on a highly-sophisticated and automatic framework for the calculation of a wide array of inorganic material properties.³⁸ The GGA-based Perdew–Burke–Ernzerhof (PBE) functional with projector-augmented wavefunction (PAW) potentials is first used within the VASP software to twice relax and optimize the ICSD-sourced structure using a 3,000-6,000 k -point mesh. The increased k -point mesh density, compared to that employed by the Materials Project, is indicative of a more computationally-expensive calculation. The band structure is then calculated with an even higher-density k -point mesh, as well as with the +U correction term for most occupied d- and f-orbital systems, and the standard band gap (E_{gap}) is extracted.³⁹ A "fitted" band gap (E_{gfit}) is then calculated by applying a standard fit, derived from a selective study of DFT-computed vs. experimentally-measured band gap widths, to the initially calculated value.⁴⁰

AFLOW-ML⁴¹, a machine learning API designed to predict thermomechanical and electronic properties based on chemical composition alone, further builds upon the entries present in the ICSD and calculated through the AFLOW framework. Using only provided atomic

compositional and positional information, so-called "fragment descriptors", the system first applies a binary metal/insulator classification model. For materials predicted to be insulators, an additional regression model is applied to predict the band gap width. Each model was subjected to a fivefold cross validation process, in which it was trained to more accurately predict properties in an independent data set. The initial binary classification model is shown to have a 93% prediction success rate, with the majority of misclassified materials being narrow-gap semiconductors. While the accuracy of the predicted band gap sizes relative to experimental values is not mentioned by the authors, roughly 93% of the machine learning-derived values are found to be within 25% of the DFT+U-calculated gap width. Only those phases identified in the authors' initial cross-validated test set were used for comparison.

4) The final stage. The criteria by which potential host species were excluded in the first three stages were largely derived computationally, with subsequent manual checks. In contrast, the final stage of screening involved the confirmation of various of the fundamental properties of the materials found in the existing literature.

First, for those remaining stoichiometries for which multiple phases appeared to be viable, the relative stability of each polymorph at STP was recorded. All recognized high-pressure and high-temperature phases that were not reported to be quenchable to a stable state under standard conditions were removed.

The intrinsic magnetic character of each pure phase was then confirmed through a combination of standard electron-counting rules and literature reports. As many of the potentially viable materials contained oxygen, particular care was taken to consider whether reported paramagnetic character could be due to oxygen-defects, especially in the various molybdate, platinate, and palladate phases. Any pure phase that was reported to deviate from diamagnetic character was removed.

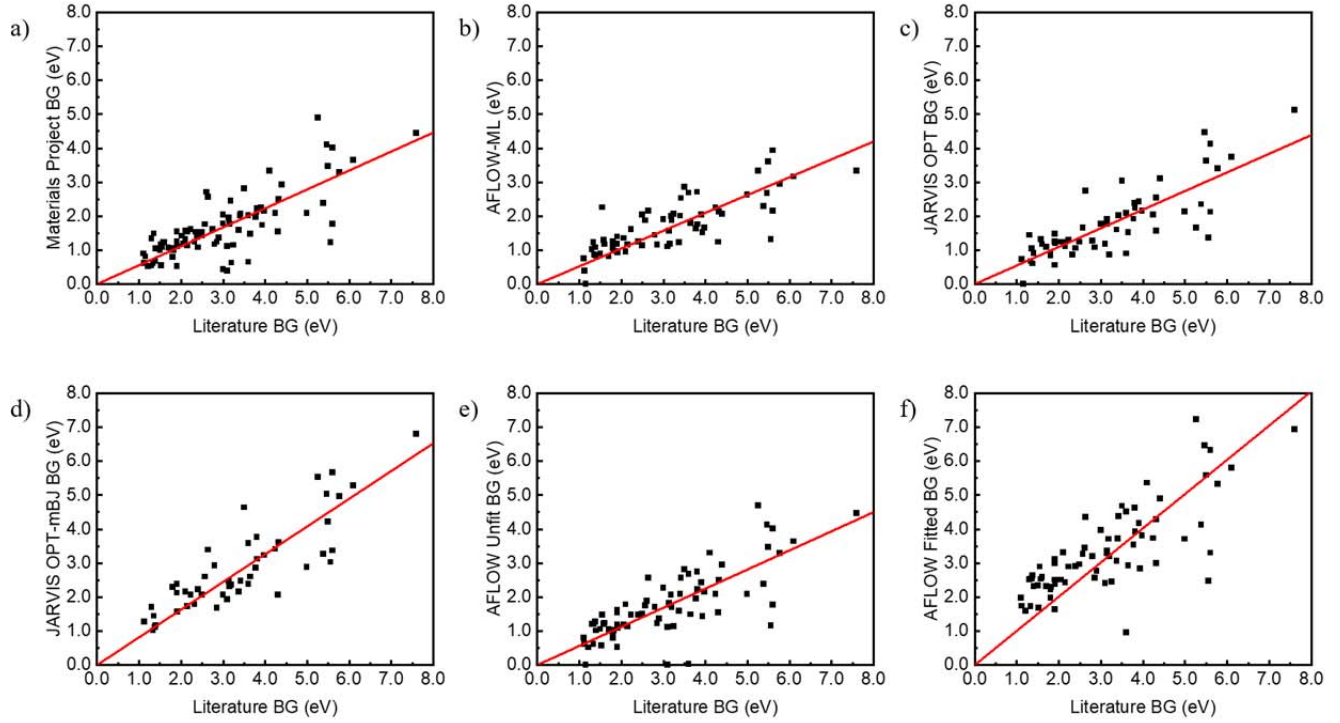


Figure 3. Comparison of reported experimental band gaps to those calculated by a) the Materials Project b) AFLOW-ML c) JARVIS-DFT (OPT only) d) JARVIS-DFT (OPT-mBJ) e) AFLOW (unfit) f) AFLOW (fit). On average, the standard DFT calculations (a, c, and e) and machine-learning predictions (b) were found to underestimate the experimental band gaps by roughly 40-50%. JARVIS-DFT OPT-mBJ calculations (d) were found to underestimate measured values by about 18% on average, while AFLOW fitted band gap calculations (f) were found to overestimate by about 2% on average, with several significant outlying underestimations. The red lines show the linear least squares fits to the data.

Where the true size of a material's band gap could not be reasonably assumed suitable based on calculations alone, other reported computationally and experimentally-derived band gap values were also taken into consideration when available. While experimental band gaps were either not available or not recorded for the majority of phases considered, those that were available were compared to the calculated values from each database, in order to better judge the viability of the selected materials with small calculated gaps (Figure 3). The standard band gap calculations performed by the Materials Project, JARVIS-DFT, and AFLOW databases were found to be underestimated by roughly 40-50%, relative to measured values, consistent with the long-known inaccuracies of DFT estimates.⁴² AFLOW-ML's machine learning-based predictions were underestimated to a similar degree. On average, the OPT-mBJ hybrid functional employed by the JARVIS-DFT database for some phases was found to reduce this underestimation to

18.4%, while the "fitted" band gap calculated by AFLOW was actually observed to be overestimated by about 1.8% relative to experimental values. However, the latter figure is heavily influenced by several outlying underestimations in the AFLOW "fitted" gap data set, suggesting that on average, band gaps calculated in this manner will be overestimated to a greater degree. The determination of band gap suitability was thus made with these findings in mind.

It should be noted that despite appearing in the literature, the most stable phases of several, long-recognized materials were found to lack an experimental crystal structure in the ICSD, and subsequently were also absent from the Materials Project database. Several of these, such as the STP-stable phases of BaGeO₃, BaGe₂O₅, and C₇₀ would be potentially viable host species, but due to their absence from any of the databases studied are not included. However, while comparing computed band gaps with reported literature values, three additional phases were identified that lacked a corresponding Materials Project entry, but did appear in at least one of the other databases. fcc-C₆₀ is the only included phase with a corresponding ICSD entry that did not appear in any of the databases considered.

While suitably-sized single crystals are necessary for the fabrication of functional devices for quantum information systems, few materials have been reported to be easily grown as large, defect-free, and optically clear single crystals. As such, the existence of published single crystal synthesis, regardless of product size, is denoted in the "SC" column in the tables of results by an asterisk. Noted air and moisture instability in the literature was also considered, but was not exclusionary, as additional post-synthesis processing may allow otherwise viable host materials to be utilized.

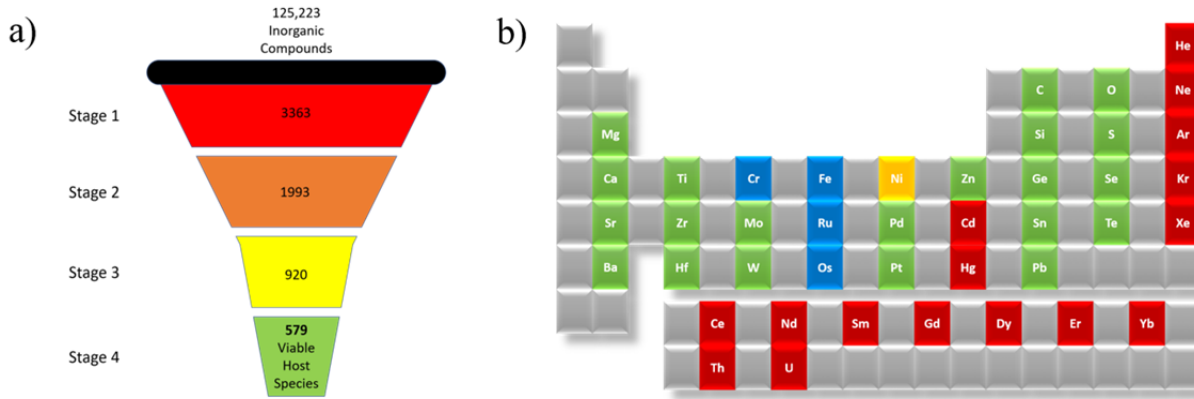


Figure 4. Tiered screening system for the identification of potentially viable host species for quantum defect implantation. a) A schematic view of the process. A maximum of 0.46% of all phases in the International Crystal Structure Database were found to be potentially viable host substrates, with the most substantial reduction in candidate phases (97.3%) occurring in Stage 1 of the screening process, b) Color-coded periodic table of constituent elements in viable host species depicting elements: disregarded due to the absence of spin-zero isotopes (gray); deemed too hazardous, too radioactive, too difficult to purify, and too unreactive for inclusion (red); not present in any identified phases (yellow); present largely only in cluster complex phases (blue); and present in numerous identified phases (green).

Of the 125,223 inorganic compounds listed in the Materials Project database, a maximum of 580 phases (0.46%) are found to fit the criteria outlined above as suitable hosts for quantum defects (Figure 4a). While there likely exist significantly more potentially viable phases that have yet to be recognized, this total spans all currently reported experimentally synthesized and theoretically predicted inorganic materials. As the ease of growth of suitably-sized single crystals, as well as stability under standard or near-standard atmospheric conditions, and chemical and structural simplicity are major factors in determining the viability of potential host phases, it is likely that those identified here represent the majority of suitable candidates.

Of the 580 identified phases, the band gap character of at least 560 could be either confirmed or reasonably assumed to be comparable or larger than that of silicon (≥ 1.1 eV), based on calculated and/or reported experimental values. The band gaps of the remaining 20 candidates, grayed in Tables 1-4, have either been reported to be slightly smaller than that of Si, or could only be tentatively extrapolated to a similar value.

Only one admitted element, Ni, was not found to be present in any of the listed phases, as all Ni-containing materials considered were found to be intrinsically paramagnetic. All the Cr-,

Fe-, and Os- containing species in the tabulations, as well as the majority of those containing Ru, are transition-metal based carbonyl cluster compounds.

Conclusion

From the total number of known, experimentally synthesized inorganic material phases, we have derived a catalog of all potentially viable host substrates for functional, atom-like defect-based quantum information systems. A combination of automatic database and subsequent manual screening was performed to ensure that each reported phase possessed the necessary electronic, magnetic, and optical properties, as well as stability under standard conditions, necessary for application in QIS. This screening was conducted across several materials databases (including the Materials Project, JARVIS-DFT, and the AFLOW repository), the AFLOW-ML prediction API, and the existing body of literature in an attempt to compensate for known computational and experimental biases and errors that may have influenced our results. Of the 580 viable candidates found, 17 are unary, 77 are binary, 337 are ternary and 149 are quaternary or higher. Many are oxides and chalcogenides, suggesting that they will be relatively simple to fabricate and study, while others in the tabulation, such as the osmates and higher order elemental clusters, will likely prove impractical for currently considered device applications. Future studies concerning inorganic material systems would likely also benefit from the implementation of similar systematic screening processes, enabling the rapid and conclusive determination of all viable phases for any number of applications.

Acknowledgements

Funding for this research was provided by the AFOSR (contract FA9550-18-1-0334), the Eric and Wendy Schmidt Transformative Technology Fund at Princeton University and the Princeton Catalysis Initiative. The authors acknowledge helpful conversations with Chris Phenicie, Paul Stevenson and Sacha Welinski.

Competing Interests

The authors declare no competing financial or non-financial interests.

Data Availability

The authors declare that the data supporting the findings of this study are available within the paper.

Author Contributions

J.D.T., N.P.dL., and R.J.C devised the main conceptual ideas and guiding principles for the project. A.M.F. performed the data screening and analysis. R.J.C. supervised the research. A.M.F. wrote the manuscript with input from all authors.

Table 1. The potentially viable unary host materials. All band gaps are reported in eV. Phases reported in the JARVIS-DFT database for which both standard OPT and hybrid OPT-mBJ calculations were performed are listed with the OPT-mBJ listed first, followed by the smaller OPT band gap in parentheses. Where the OPT-mBJ-computed band gap was found to be unrealistically small, compared to the basic OPT-calculated one, only the OPT-computed band gap is listed. Where multiple AFLOW repository entries were found to exist for the same phase of a compound, the average of each computed band gap size is listed. Literature band gaps listed in bold correspond to those experimentally-derived, while those not bolded correspond to reported, alternatively calculated band gap widths, many of which are seen to agree with the database DFT-calculations. The presence of * in the SC column denotes a known single-crystal synthesis method for that particular phase. (-) in any cell corresponds to uncalculated and unreported values for that particular phase, respectively.

Entry #	Materials ID	Formula	Space Group	Band Gap (eV)					SC
				Materials Project	AFLOW-ML	Jarvis OPT-mBJ (OPT)	AFLOW $E_{gfit}(E_{gap})$	Literature	
1	mp-66	C (diamond)	Fd $\bar{3}$ m	4.11	2.67	5.04 (4.46)	6.46 (4.12)	5.47 ⁴³	*
2	-	C ₆₀	Fm $\bar{3}$ m	-	-	-	-	1.86 ⁴⁴	*
3	mp-557031	S ₆ S ₁₀	C2/c	2.05	2.44	-	2.90 (1.47)	-	*
4	mp-77	α -S ₈	Fddd	2.71	insulator	-	3.44 (1.88)	2.61 ⁴⁵	*
5	mp-558014	S ₁₂	Pnnm	2.46	2.31	-	4.19 (2.43)	-	*
6	mp-583072	S ₁₃	P2 ₁ /c	2.44	-	-	-	-	*
7	mp-561513	S ₁₄	P $\bar{1}$	2.43	2.54	-	4.28 (2.50)	-	*
8	mp-555915	α -S ₁₈	P2 ₁ 2 ₁ 2 ₁	2.54	-	-	-	-	*
9	mp-558964	S ₂₀	Pbcn	2.54	-	-	-	-	*
10	mp-14	Se	P3 ₁ 21	1.06	1.07	2.29 (0.90)	2.23 (0.98)	1.80 ⁴⁶	*
11	mp-147	Se ₆	R $\bar{3}$	1.54	1.18	2.12 (1.25)	3.00 (1.55)	1.90 ⁴⁶	*
12	mp-570481	γ -Se ₈	P2 ₁ /c	1.66	1.00	-	3.09 (1.62)	-	*
13	mp-542605	β -Se ₈	P2 ₁ /c	1.39	-	1.98 (1.12)	3.28 (1.76)	-	*
14	mp-542461	α -Se ₈	P2 ₁ /c	1.57	0.95	2.16 (1.24)	3.31 (1.78)	2.10 ⁴⁶	*
15	mp-149	Si	Fd $\bar{3}$ m	0.62	0.38	1.28 (0.73)	1.74 (0.61)	1.12 ⁴⁷	*
16	mp-1095269	Si ₂₄	Cmcm	0.54	-	-	-	1.29 ⁴⁸	
17	mp-16220	Si ₁₃₆	Fd $\bar{3}$ m	0.53	-	0.56	1.63 (0.53)	1.90 ⁴⁹	

Table 2. The potentially viable binary host materials. All band gaps are reported in eV. Phases reported in the JARVIS-DFT database for which both standard OPT and hybrid OPT-mBJ calculations were performed are listed with the OPT-mBJ listed first, followed by the smaller OPT band gap in parentheses. Where the OPT-mBJ-computed band gap was found to be unrealistically small, compared to the basic OPT-calculated one, only the OPT-computed band gap is listed. Where multiple AFLOW repository entries were found to exist for the same phase of a compound, the average of each computed band gap size is listed. Literature band gaps listed in bold correspond to those experimentally-derived, while those not bolded correspond to reported, alternatively calculated band gap widths, many of which are seen to agree with the database DFT-calculations. The presence of * in the SC column denotes a known single-crystal synthesis method for that particular phase. (-) in any cell corresponds to uncalculated and unreported values for that particular phase, respectively. Grayed text indicates materials where the band gap is considered to be near enough to that of elemental Si to be potentially viable.

				Band Gap (eV)					
Entry #	Materials ID	Formula	Space Group	Materials Project	AFLOW-ML	Jarvis OPT-mBJ (OPT)	AFLOW $E_{gfit}(E_{gap})$	Literature	SC
18	mp-1735	BaC ₂	I4/mmm	1.62	1.47	3.09 (1.79)	3.09 (1.61)	2.20 ⁵⁰	*
19	mp-1342	BaO	Fm $\bar{3}$ m	2.09	2.24	3.41 (2.05)	3.73 (2.09)	4.10-4.38 ⁵¹	*
20	mp-1105	BaO ₂	I4/mmm	2.24	2.71	3.74 (2.33)	3.92 (2.23)	-	*
21	mp-1500	BaS	Fm $\bar{3}$ m	2.16	1.66	3.23 (2.15)	3.81 (2.15)	3.90-4.05 ⁵¹	*
22	mp-684	BaS ₂	C2/c	1.58	1.48	2.59 (1.63)	3.03 (1.57)	-	*
23	mp-239	BaS ₃	P $\bar{4}2_1$ m	1.37	1.23	1.02	2.76 (1.37)	-	*
24	mp-1253	BaSe	Fm $\bar{3}$ m	1.96	1.63	2.85 (1.92)	3.54 (1.95)	3.60-3.95 ⁵¹	*
25	mp-7547	BaSe ₂	C2/c	0.74	1.05	0.68	1.75 (0.62)	-	*
26	mp-7548	BaSe ₃	P $\bar{4}2_1$ m	0.93	0.99	1.93 (1.00)	2.17 (0.93)	-	
27	mp-1477	BaSi ₂	Pnma	0.81	metal	metal	metal	1.15 ⁵²	*
28	mp-1000	BaTe	Fm $\bar{3}$ m	1.59	1.23	2.15 (1.60)	3.06 (1.59)	3.10-3.65 ⁵¹	*
29	mp-8234	BaTe ₃	P $\bar{4}2_1$ m	0.81	0.50	1.29 (0.76)	1.90 (0.74)	-	*
30	mp-1197923	C ₆₁ O ₂	P2 ₁ /c	1.29	-	-	-	-	
31	mp-1203337	C ₃ S ₄	P2 ₁ /c	1.47	-	-	-	-	*
32	mp-30078	C ₃ S ₈	P $\bar{3}$	1.73	2.37	-	3.21 (1.70)	-	*
33	mp-27814	CS ₁₄	R $\bar{3}$ m	2.54	2.17	3.23 (2.28)	4.28 (2.50)	-	*
34	mp-2482	CaC ₂	I4/mmm	1.35	1.90	2.62 (1.44)	2.70 (1.32)	-	*
35	mp-2605	CaO	Fm $\bar{3}$ m	3.65	3.16	5.29 (3.74)	5.81 (3.64)	6.10 ⁵³	*

36	mp-634859	CaO ₂	I4/mmm	2.73	3.24	4.22 (2.98)	4.58 (2.72)	2.50 ⁵⁴	
37	mp-1672	CaS	Fm $\bar{3}$ m	2.39	2.29	3.27 (2.35)	4.13 (2.39)	5.38 ⁵¹	*
38	mp-1415	CaSe	Fm $\bar{3}$ m	2.09	2.63	2.88 (2.14)	3.71 (2.08)	4.87-5.11 ⁵¹	*
39	mp-1519	CaTe	Fm $\bar{3}$ m	1.55	1.24	2.06 (1.56)	2.99 (1.54)	4.07-4.55 ⁵¹	
40	mp-470	GeO ₂	P4 ₂ /mnmm	1.23	1.31	3.03 (1.37)	2.48 (1.16)	5.56 ⁵⁵	*
41	mp-2242	GeS	Pnma	1.24	1.30	1.32	2.53 (1.20)	1.58 ⁵⁶	*
42	mp-700	GeSe	Pnma	0.90	0.75	-	1.98 (0.79)	1.10 ⁵⁷	*
43	mp-10074	GeSe ₂	I $\bar{4}2d$	1.52	1.13	2.06 (1.24)	2.96 (1.51)	2.49 ⁵⁸	*
44	mp-352	HfO ₂	P2 ₁ /c	4.02	3.93	5.66 (4.12)	6.33 (4.02)	5.60 ⁵⁹	*
45	mp-985829	HfS ₂	P $\bar{3}$ m1	1.24	1.16	1.68 (1.08)	2.57 (1.23)	2.85 ⁶⁰	*
46	mp-9922	HfS ₃	P2 ₁ /m	1.12	1.10	1.93 (1.18)	2.41 (1.11)	3.10 ⁶¹	*
47	mp-29771	MgC ₂	P4 ₂ /mnmm	2.57	2.15	3.39 (2.75)	4.36 (2.56)	2.64 ⁶²	
48	mp-28793	Mg ₂ C ₃	Pnnm	1.65	2.12	2.41 (1.74)	3.16 (1.67)	2.09 ⁶³	
49	mp-1265	MgO	Fm $\bar{3}$ m	4.45	3.34	6.80 (5.13)	6.94 (4.47)	7.60 ⁵¹	*
50	mp-1315	MgS	Fm $\bar{3}$ m	2.79	3.04	4.26 (2.94)	4.65 (2.77)	3.0+ ⁶⁴	*
51	mp-10760	MgSe	Fm $\bar{3}$ m	1.77	2.16	3.37 (2.12)	3.30 (1.77)	5.60 ⁵¹	
52	mp-1103590	MgSe ₂	Pa $\bar{3}$	1.63	1.57	-	3.12 (1.64)	3.62 ⁶⁵	
53	mp-20589	MoO ₃	Pnma	1.95	1.57	2.46 (1.92)	3.37 (1.82)	3.14 ⁶⁶	*
54	mp-1018809	MoS ₂	P6 ₃ /mmc	1.34	1.02	1.7 (1.44)	2.52 (1.20)	1.30 ⁶⁷	*
55	mp-1634	MoSe ₂	P6 ₃ /mmc	1.46	0.85	1.62 (1.49)	2.41 (1.12)	1.41 ⁶⁸	*
56	mp-19921	PbO	P4/nmm	1.53	0.95	2.39 (1.47)	3.10 (1.62)	1.90 ⁶⁹	*
57	mp-608439	Pb ₂ O ₃	P2 ₁ /m	1.07	0.81	1.09	2.31 (1.04)	1.70 ⁷⁰	
58	mp-22633	Pb ₃ O ₄	P4 ₂ /mbc	1.14	1.16	1.73 (1.10)	2.43 (1.13)	2.10-2.20 ⁷⁰	*
59	mp-1285	PtO ₂	Pnnm	0.60	0.95	-	2.08 (0.68)	-	*
60	mp-2030	RuS ₂	Pa $\bar{3}$	0.67	1.08	1.11 (0.60)	2.63 (1.28)	1.38 ⁷¹	*
61	mp-726	SeO ₂	P4 ₂ /mbc	3.28	2.89	3.42	5.29 (3.25)	-	*
62	mp-27519	SeO ₃	P $\bar{4}2_1$ c	2.43	-	-	4.16 (2.41)	-	
63	mp-27358	Se ₂ O ₅	P2 ₁ /c	2.89	2.96	-	4.81 (2.89)	-	*
64	mp-8062	SiC (3C)	F $\bar{4}3$ m	1.39	-	-	-	2.39 ⁷²	*
65	mp-640917	SiO ₂	P3 ₂ 121	0.66	-	-	-	9.65 ⁷³	*
66	mp-1602	SiS ₂	Ibam	3.07	2.58	3.56 (2.73)	5.00 (3.03)	2.44 ⁷⁴	*
67	mp-568264	SiSe ₂	Ibam	2.16	1.92	2.51 (1.61)	3.64 (2.02)	3.35 ⁷⁴	*
68	mp-856	SnO ₂	P4 ₂ /mnmm	0.65	-	2.38 (0.90)	0.95 (0.03)	3.60 ⁷⁵	*

69	mp-2231	SnS	Pnma	0.95	-	1.47 (1.02)	2.16 (0.93)	1.11 ⁷⁶	*
70	mp-1509	Sn ₂ S ₃	Pnma	0.78	0.92	-	1.81 (0.67)	1.09 ⁷⁶	*
71	mp-2630	SrC ₂	I4/mmm	1.67	1.48	3.05 (1.80)	3.17 (1.67)	-	
72	mp-2472	SrO	Fm $\bar{3}$ m	3.29	2.94	4.96 (3.40)	5.33 (3.28)	5.77 ⁵¹	*
73	mp-2697	SrO ₂	I4/mmm	2.86	3.04	4.25 (3.10)	4.71 (2.82)	-	
74	mp-1087	SrS	Fm $\bar{3}$ m	2.50	2.14	3.61 (2.54)	4.28 (2.50)	4.32 ⁵¹	*
75	mp-1950	SrS ₂	I4/mcm	1.29	1.81	2.72 (1.58)	2.63 (1.28)	-	*
76	mp-2758	SrSe	Fm $\bar{3}$ m	2.23	1.76	3.12 (2.24)	3.92 (2.23)	3.81 ⁵¹	*
77	mp-1958	SrTe	Fm $\bar{3}$ m	1.77	1.18	2.31 (1.77)	3.29 (1.76)	2.90-3.40 ⁷⁷	*
78	mp-2125	β -TeO ₂	Pbca	2.23	2.80	3.76 (2.18)	3.92 (2.23)	2.20 ⁷⁸	
79	mp-557	α -TeO ₂	P4 ₁ 2 ₁ 2	2.81	2.86	4.64 (3.04)	4.68 (2.81)	3.50 ⁷⁹	*
80	mp-2552	TeO ₃	R $\bar{3}$ c	1.15	2.06	-	2.45 (1.14)	3.25 ⁸⁰	
81	mp-390	TiO ₂ (anatase)	I4 ₁ /amd	2.06	2.53	2.47 (2.02)	4.37 (2.56)	3.42 ⁸¹	*
82	mp-2657	TiO ₂ (rutile)	P4 ₂ /mnM	1.78	1.91	2.07 (1.77)	3.97 (2.27)	3.00 ⁸²	*
83	mp-619461	γ -WO ₃	P2 ₁ /c	1.37	-	-	2.76 (1.37)	2.60-3.2 ⁸³	*
84	mp-1197857	δ -WO ₃	P $\bar{1}$	1.67	-	-	2.94 (1.50)	-	*
85	mp-1821	WSe ₂	P6 ₃ /mmc	1.49	0.87	1.44 (1.05)	2.54 (1.21)	1.35 ⁸⁴	*
86	mp-1986	ZnO	F $\bar{4}3$ m	0.63	1.88	2.36 (0.87)	3.19 (1.69)	3.20 ⁸⁵	*
87	mp-8484	ZnO ₂	Pa $\bar{3}$	2.13	2.71	3.76 (2.38)	4.62 (2.75)	3.80 ⁸⁵	
88	mp-10695	ZnS	F $\bar{4}3$ m	2.02	2.69	3.59 (2.09)	4.52 (2.68)	3.60 ⁸⁶	*
89	mp-1102743	ZnS ₂	Pa $\bar{3}$	1.43	2.05	-	-	2.50 ⁸⁷	
90	mp-1190	ZnSe	F $\bar{4}3$ m	1.17	1.44	2.92 (1.27)	3.20 (1.70)	2.80 ⁸⁸	*
91	mp-2176	ZnTe	F $\bar{4}3$ m	1.08	1.25	2.23 (1.06)	2.90 (1.47)	2.40 ⁸⁸	*
92	mp-2858	ZrO ₂	P2 ₁ /c	3.47	3.61	4.21 (3.62)	5.59 (3.47)	5.00-6.00 ⁸⁹	*
93	mp-1186	ZrS ₂	P $\bar{3}$ m1	1.05	0.85	1.17 (0.91)	2.32 (1.01)	1.40 ⁹⁰	*
94	mp-9921	ZrS ₃	P2 ₁ /m	1.10	0.93	1.56 (1.21)	2.38 (1.09)	1.91 ⁹¹	*

Table 3. The potentially viable ternary host materials. All band gaps are reported in eV. Phases reported in the JARVIS-DFT database for which both standard OPT and hybrid OPT-mBJ calculations were performed are listed with the OPT-mBJ listed first, followed by the smaller OPT band gap in parentheses. Where the OPT-mBJ-computed band gap was found to be unrealistically small, compared to the basic OPT-calculated one, only the OPT-computed band gap is listed. Where multiple AFLOW repository entries were found to exist for the same phase of a compound, the average of each computed band gap size is listed. Literature band gaps listed in bold correspond to those experimentally-derived, while those not bolded correspond to reported, alternatively calculated band gap widths, many of which are seen to agree with the database DFT-calculations. The presence of * in the SC column denotes a known single-crystal synthesis method for that particular phase. (-) in any cell corresponds to uncalculated and unreported values for that particular phase, respectively. Grayed text indicates shows materials where the band gap is considered to be near enough to that of elemental Si to be potentially viable.

				Band Gap (eV)					
Entry #	Materials ID	Formula	Space Group	Materials Project	AFLOW-ML	Jarvis OPT-mBJ (OPT)	AFLOW $E_{gfit}(E_{gap})$	Literature	SC
95	mp-5504	BaCO ₃	Pnma	4.38	-	-	-	-	*
96	-	BaC ₂ O ₄	P ₁	-	3.43	-	5.29 (3.25)	-	*
97	mp-30237	Ba(CO) ₄	I4/mcm	2.61	2.95	3.87 (2.67)	4.37 (2.56)	-	*
98	mp-18571	BaCrO ₄	Pnma	2.96	2.76	-	4.86 (2.93)	-	*
99	mp-572430	BaCr ₂ O ₇	C2/c	2.63	-	-	-	-	
100	mp-3848	BaGe ₄ O ₉	P321	3.05	-	-	4.97 (3.01)	-	*
101	mp-1195469	BaGeS ₃	P2 ₁ /c	2.40	-	-	-	-	*
102	mp-28710	BaGe ₂ S ₅	Fd ₃ m	2.19	-	2.09	3.83 (2.16)	-	*
103	mp-540805	Ba ₂ GeS ₄	Pnma	2.29	2.37	-	3.93 (2.24)	2.39 ⁹²	*
104	mp-1200759	Ba ₃ GeS ₅	Pnma	2.04	-	-	-	3.00 ⁹³	*
105	mp-11902	Ba ₂ GeSe ₄	P2 ₁ /m	1.40	1.45	1.26	2.77 (1.38)	3.00 ⁹⁴	*
106	mp-18335	Ba ₂ Ge ₂ Se ₅	Pnma	1.29	1.36	-	2.62 (1.27)	1.60 ⁹⁵	*
107	mp-1105549	BaHfS ₃	Pnma	1.24	-	1.78 (0.86)	-	2.32 ⁹⁶	
108	mp-9321	Ba ₂ HfS ₄	I4/mmm	0.88	1.38	1.43 (0.91)	2.08 (0.87)	1.58 ⁹⁷	*
109	mp-1189858	Ba ₄ Hf ₃ S ₁₀	I4/mmm	0.74	0.41	-	metal	-	*
110	mp-557032	Ba ₅ Hf ₄ S ₁₃	I4/mmm	0.64	0.45	0.61	-	-	*
111	mp-554688	Ba ₆ Hf ₅ S ₁₆	I4/mmm	0.60	0.37	0.67	-	-	*
112	mp-19276	BaMoO ₄	I4 ₁ /a	4.15	3.13	-	6.24 (3.95)	-	*

113	mp-20098	Ba ₂ PbO ₄	I4/mmm	1.22	1.55	-	2.57 (1.23)	1.70 ⁹⁸	*
114	mp-4009	BaPdS ₂	Cmcm	0.38	1.08	0.16 (0.13)	2.10 (0.88)	-	*
115	mp-28967	Ba(PdS ₂) ₂	P2 ₁ /m	0.90	1.08	1.11 (0.97)	2.37 (1.08)	-	*
116	mp-8727	Ba ₄ PtO ₆	R̄3c	1.80	2.20	1.84	3.61 (2.00)	-	
117	mp-29787	Ba ₅ Pt ₂ O ₉	P321	1.93	-	-	3.85 (2.18)	-	
118	mp-29289	BaPt ₂ S ₃	P4 ₁ 2 ₁ 2	0.97	1.39	-	2.64 (1.28)	-	*
119	mp-3164	BaSO ₄	Pnma	5.95	5.73	6.49	8.94 (5.97)	-	*
120	mp-1019557	BaS ₄ O ₁₃	C2/c	4.68	-	-	-	-	
121	mp-6989	BaSeO ₃	P2 ₁ /m	3.90	3.52	3.98	6.14 (3.88)	-	*
122	mp-12010	BaSeO ₄	Pnma	3.70	3.62	-	5.89 (3.69)	-	*
123	mp-28536	BaSe ₂ O ₅	P2 ₁ /c	3.37	3.09	-	5.47 (3.38)	-	*
124	mp-7339	BaSiO ₃	P2 ₁ 2 ₁ 2 ₁	4.53	3.91	-	7.02 (4.53)	-	*
125	mp-3031	BaSi ₂ O ₅	Pnma	4.76	4.48	-	6.85 (4.40)	-	*
126	mp-9478	BaSi ₄ O ₉	P̄6c2	4.35	4.31	4.50	6.78 (4.35)	-	*
127	mp-17612	Ba ₂ SiO ₄	Pnma	4.63	-	-	-	-	
128	mp-29222	Ba ₂ Si ₃ O ₈	P2 ₁ /c	4.51	-	-	7.00 (4.52)	-	*
129	mp-7765	Ba ₃ SiO ₅	I4/mcm	3.54	3.24	3.46	5.67 (3.53)	-	
130	mp-669333	Ba ₅ Si ₈ O ₂₁	C2/c	4.50	-	-	-	-	*
131	mp-5838	Ba ₂ SiS ₄	Pnma	3.00	2.70	-	4.97 (3.01)	-	*
132	mp-27805	Ba ₃ SiS ₅	Pnma	2.81	2.57	-	4.70 (2.81)	-	
133	mp-14447	Ba ₂ SiSe ₄	P2 ₁ /m	2.28	1.67	2.30	3.97 (2.27)	3.95 ⁹⁴	*
134	mp-14448	Ba ₂ SiTe ₄	P2 ₁ /m	1.10	0.92	1.09	2.40 (1.10)	-	*
135	mp-3163	BaSnO ₃	Pm̄3m	0.38	-	-	metal	3.10⁹⁹	*
136	mp-3359	Ba ₂ SnO ₄	I4/mmm	2.45	2.00	-	3.71 (2.07)	3.18¹⁰⁰	
137	mp-12181	BaSnS ₂	P2 ₁ /c	1.62	1.38	1.76	3.17 (1.68)	2.40 ¹⁰¹	*
138	mp-27802	BaSn ₂ S ₃	P2 ₁ /m	1.35	1.41	-	2.61 (1.26)	-	*
139	mp-1202711	BaSn ₂ S ₅	Pccn	1.53	-	-	-	2.35¹⁰²	*
140	mp-541832	Ba ₂ SnS ₄	P2 ₁ /c	1.96	1.90	-	3.18 (1.68)	-	
141	mp-556291	Ba ₃ Sn ₂ S ₇	P2 ₁ /c	2.19	1.84	-	3.55 (1.96)	-	*
142	mp-1204773	Ba ₆ Sn ₇ S ₂₀	C2/c	1.45	-	-	-	-	*
143	mp-1192595	Ba ₂ SnSe ₄	P2 ₁ /c	1.26	-	-	-	1.90¹⁰³	*
144	mp-31307	Ba ₂ SnSe ₅	P2 ₁ 2 ₁ 2 ₁	1.08	-	-	-	1.20¹⁰⁴	*
145	mp-1196224	Ba ₆ Sn ₆ Se ₁₃	P2 ₁ 2 ₁ 2 ₁	1.16	-	-	-	1.52¹⁰⁵	*

146	mp-569754	$\text{Ba}_7\text{Sn}_3\text{Se}_{13}$	Pnma	1.41	-	-	-	-	$1.60\text{-}2.00^{106}$	*
147	mp-5431	BaTeO_3	P2 ₁ /m	2.71	-	-	-	-	-	*
148	mp-556021	BaTeO_3	Pnma	3.17	-	-	-	-	-	*
149	mp-27254	$\text{Ba}(\text{TeO}_3)_2$	Cmcm	1.76	2.27	2.54 (1.91)	3.26 (1.74)	2.10^{107}		
150	mp-1195118	BaTe_3O_7	P2 ₁ /c	3.26	-	-	-	-	-	*
151	mp-1195016	BaTe_4O_9	C2/c	3.18	-	-	-	-	-	*
152	mp-1078191	Ba_2TeO	P4/nmm	1.78	-	-	-	2.93^{108}	*	
153	mp-17009	$\text{Ba}_3\text{Te}_2\text{O}_9$	P6 ₃ /mmc	2.37	2.62	-	4.09 (2.36)	-		
154	mp-28102	$\text{Ba}_3\text{Te}_4\text{O}_{11}$	P $\bar{1}$	3.22	-	-	-	-	-	*
155	mp-27499	BaTeS_3	Pnma	1.91	1.67	-	3.49 (1.91)	-	-	*
156	mp-3175	BaTi_4O_9	Pmmn	2.79	2.50	-	5.22 (3.20)	-	-	*
157	mp-27790	$\text{BaTi}_5\text{O}_{11}$	P2 ₁ /c	2.70	-	-	-	-	-	*
158	mp-504457	$\text{BaTi}_6\text{O}_{13}$	P $\bar{1}$	2.64	2.50	-	4.85 (2.92)	-	-	*
159	mp-3397	Ba_2TiO_4	P2 ₁ /c	4.15	2.93	-	-	-	-	*
160	mp-560731	$\text{Ba}_2\text{Ti}_9\text{O}_{20}$	P $\bar{1}$	2.74	-	-	-	-	-	*
161	mp-29298	$\text{Ba}_4\text{Ti}_{13}\text{O}_{30}$	Cmce	2.59	-	-	-	-	-	*
162	mp-556729	$\text{Ba}_6\text{Ti}_{17}\text{O}_{40}$	C2/c	2.71	-	-	-	-	-	*
163	mp-17908	Ba_2TiS_4	Pnma	2.10	1.64	-	3.75 (2.11)	-		
164	mp-9668	Ba_3TiS_5	I4/mcm	1.45	1.51	1.38	2.77 (1.38)	-		
165	mp-19048	BaWO_4	I4 ₁ /a	4.89	3.34	5.53 (1.66)	7.23 (4.69)	5.26^{109}	*	
166	mp-28403	Ba_2WO_5	Pnma	3.15	3.13	-	4.79 (2.87)	-		
167	mp-22086	Ba_3WO_6	Fm $\bar{3}$ m	2.99	3.03	-	4.58 (2.72)	-	-	*
168	mp-18867	$\text{Ba}_3\text{W}_2\text{O}_9$	R $\bar{3}$ c	3.67	-	-	5.56 (3.45)	-		
169	mp-4236	BaZnO_2	P3 ₁ 21	2.27	2.48	3.92 (2.50)	4.66 (2.78)	2.20^{110}	*	
170	mp-17911	Ba_2ZnO_3	C2/c	2.67	2.53	-	5.09 (3.10)	-	-	*
171	mp-5587	Ba_2ZnS_3	Pnma	2.02	2.01	-	3.72 (2.08)	3.31 - 3.49 ¹¹¹	*	
172	mp-1190528	Ba_2ZnSe_3	Pnma	1.62	-	-	-	2.75 ¹¹²	*	
173	mp-1190380	Ba_2ZnTe_3	Pnma	1.32	-	-	-	2.10 ¹¹³	*	
174	mp-3834	BaZrO_3	Pm $\bar{3}$ m	3.05	2.81	3.84 (3.25)	5.00 (3.04)	-		
175	mp-8335	Ba_2ZrO_4	I4/mmm	2.99	3.00	-	4.93 (2.98)	-		
176	mp-540771	BaZrS_3	Pnma	1.00	0.97	-	2.29 (1.02)	1.82 ⁹⁷	*	
177	mp-3813	Ba_2ZrS_4	I4/mmm	0.62	1.23	1.01 (0.67)	1.73 (0.61)	1.33 ⁹⁷	*	
178	mp-9179	$\text{Ba}_3\text{Zr}_2\text{S}_7$	I4/mmm	0.52	-	-	1.59 (0.51)	1.21 ⁹⁷	*	

179	mp-14883	Ba ₄ Zr ₃ S ₁₀	I4/mmm	0.47	0.84	-	1.54 (0.47)	-	*
180	mp-560839	C ₄ SeO ₂	Pnnm	1.43	-	-	2.92 (1.49)	-	
181	mp-553939	CaCO ₃	Pnma	4.70	-	6.44 (4.78)	6.53 (4.17)	-	
182	mp-3953	CaCO ₃	R <bar>3}c</bar>	5.00	4.50	6.90 (5.17)	7.65 (5.00)	-	*
183	mp-558543	Ca(CO ₂) ₂	P2/m	3.12	4.02	-	5.13 (3.13)	-	
184	mp-19215	CaCrO ₄	I4 ₁ /amd	2.37	2.10	2.59 (2.16)	4.06 (2.34)	2.16 ¹¹⁴	*
185	mp-8130	CaGeO ₃	Pnma	2.03	-	2.17	-	-	*
186	mp-554678	CaGe ₂ O ₅	P <bar>1}</bar>	2.46	2.51	2.60	-	-	*
187	mp-560647	Ca ₂ GeO ₄	Pnma	3.60	-	3.71	5.72 (3.57)	-	*
188	mp-29273	Ca ₂ Ge ₇ O ₁₆	P <bar>4}b2</bar>	2.87	2.79	-	-	-	*
189	mp-774105	Ca ₅ Ge ₃ O ₁₁	P <bar>1}</bar>	3.35	3.02	-	-	-	*
190	mp-540773	Ca ₂ GeS ₄	Pnma	2.52	2.44	-	4.28 (2.49)	-	
191	mp-754853	CaHfO ₃	Pnma	4.49	-	4.57	-	-	*
192	mp-558164	CaHf ₄ O ₉	C2/c	4.45	-	-	6.91 (4.45)	-	
193	mp-27221	Ca ₂ Hf ₇ O ₁₆	R <bar>3}</bar>	4.31	3.74	-	6.73 (4.32)	-	
194	mp-558489	Ca ₆ Hf ₁₉ O ₄₄	R <bar>3}c</bar>	4.13	-	-	-	-	
195	mp-1190098	CaHfS ₃	Pnma	1.52	-	-	-	2.21 ⁹⁶	
196	mp-19330	CaMoO ₄	I4 ₁ /a	3.51	2.93	-	5.42 (3.34)	-	*
197	mp-20079	CaPbO ₃	Pnma	0.93	-	1.62 (0.96)	-	-	
198	mp-21137	Ca ₂ PbO ₄	Pbam	1.48	1.79	2.6 (1.52)	2.92 (1.49)	3.65 ¹¹⁵	*
199	mp-10299	Ca ₄ PdO ₆	R <bar>3}c</bar>	1.79	1.94	1.98 (1.82)	3.62 (2.03)	-	
200	mp-4784	CaPtO ₃	Cmcm	1.27	1.61	1.45 (1.36)	3.10 (1.62)	-	
201	mp-8710	Ca ₂ Pt ₃ O ₈	R <bar>3}m</bar>	1.08	1.52	-	3.09 (1.61)	-	
202	mp-8568	Ca ₄ PtO ₆	R <bar>3}c</bar>	2.38	2.20	2.64 (2.41)	4.51 (2.67)	-	*
203	mp-4406	CaSO ₄	Cmcm	5.94	-	6.47	-	-	*
204	mp-1019581	CaS ₃ O ₁₀	P2 ₁ /c	4.92	-	-	-	-	
205	mp-557997	CaSeO ₃	P2 ₁ /c	4.23	-	6.02 (4.36)	-	-	*
206	mp-1190360	CaSeO ₄	P2 ₁ /c	3.38	-	-	5.54 (3.43)	-	*
207	mp-27845	CaSe ₂ O ₅	Pbca	3.48	3.41	-	5.61 (3.49)	-	*
208	mp-28535	Ca ₂ Se ₃ O ₈	P <bar>1}</bar>	3.42	3.48	-	-	-	*
209	mp-5733	CaSiO ₃	P2 ₁ /c	4.88	-	5.17	-	-	
210	mp-561086	CaSiO ₃	C2/c	4.71	-	-	7.27 (4.72)	-	*
211	mp-4428	CaSiO ₃	P <bar>1}</bar>	4.73	-	-	7.29 (4.73)	-	

212	mp-556942	Ca ₂ SiO ₄	P2 ₁ /c	4.45	4.19	-	6.86 (4.41)	-	
213	mp-4481	Ca ₂ SiO ₄	Pnma	4.20	-	-	5.87 (3.68)	-	*
214	mp-641754	Ca ₃ SiO ₅	P $\bar{1}$	3.99	-	-	-	-	*
215	mp-3932	Ca ₃ Si ₂ O ₇	P2 ₁ /c	4.43	-	-	-	-	
216	mp-1019570	Ca ₈ Si ₅ O ₁₈	Pbcn	4.55	-	-	-	-	
217	-	Ca ₂ SiS ₄	Pnma	-	2.96	-	5.09 (3.10)	-	
218	mp-1194183	Ca ₂ SiSe ₄	Pnma	2.47	2.00	-	4.15 (2.40)	-	
219	mp-4438	CaSnO ₃	Pnma	2.33	-	-	-	3.80-4.96 ¹¹⁶	*
220	mp-4190	CaSnO ₃	R $\bar{3}$	2.92	2.07	3.11	4.89 (2.95)	4.40 ¹¹⁷	
221	mp-4747	Ca ₂ SnO ₄	Pbam	2.72	2.22	4.66 (2.89)	4.23 (2.46)	-	
222	mp-866503	Ca ₂ SnS ₄	Pnma	2.26	2.07	1.74 (0.73)	3.68 (2.05)	-	*
223	mp-12221	CaTeO ₄	Pbcn	2.25	2.49	2.33	3.96 (2.26)	-	
224	mp-5040	CaTe ₂ O ₅	P2 ₁ /c	3.37	2.66	3.29	5.43 (3.35)	-	*
225	mp-15511	CaTe ₃ O ₈	C2/c	2.04	2.32	-	3.61 (2.00)	-	*
226	mp-5279	Ca ₃ TeO ₆	P2 ₁ /c	3.25	2.44	4.56 (3.47)	3.26 (1.74)	-	*
227	mp-680711	Ca ₄ Te ₅ O ₁₄	Pbca	2.86	-	-	-	-	*
228	mp-559210	Ca ₅ Te ₃ O ₁₄	Cmce	1.70	2.36	-	-	-	
229	mp-4019	CaTiO ₃	Pnma	2.32	2.66	2.82 (2.31)	4.81 (2.89)	-	*
230	mp-19426	CaWO ₄	I4 ₁ /a	4.34	3.61	-	6.43 (4.10)	-	*
231	mp-779906	Ca ₃ WO ₆	P2 ₁ /c	3.55	-	-	-	-	
232	mp-4571	CaZrO ₃	Pnma	3.83	3.16	4.05	6.06 (3.82)	-	*
233	mp-554190	CaZr ₄ O ₉	C2/c	3.84	-	-	6.09 (3.84)	-	*
234	mp-7781	CaZrS ₃	Pnma	1.19	1.40	-	2.51 (1.19)	1.90 ¹¹⁸	
235	mp-647812	Cr(CO) ₆	Pnma	3.46	2.93	-	5.81 (3.63)	-	*
236	mp-19146	CrPbO ₄	P2 ₁ /c	2.05	2.00	-	metal	-	*
237	mp-22373	CrPb ₂ O ₅	C2/m	1.82	1.97	-	3.46 (1.89)	-	*
238	mp-705034	CrPb ₅ O ₈	P2 ₁ /c	1.88	-	-	-	-	*
239	mp-643081	Fe ₂ (CO) ₉	P6 ₃ /m	2.48	3.05	-	4.42 (2.60)	-	
240	mp-553898	GePbO ₃	P2/c	2.70	-	-	-	-	*
241	mp-583345	GePb ₅ O ₇	Pbca	2.17	-	-	-	-	*
242	mp-29217	Ge ₃ PbO ₇	Pbca	2.65	-	-	-	-	*
243	mp-680143	Ge ₃ Pb ₁₁ O ₁₇	P $\bar{1}$	2.14	-	-	-	-	
244	mp-624190	GePbS ₃	P2 ₁ /c	1.76	1.87	2.60 (1.66)	3.27 (1.75)	2.57 ¹¹⁹	*

245	mp-560370	Ge(PbS ₂) ₂	P2 ₁ /c	2.02	1.67	2.78 (1.93)	3.60 (2.00)	-	*
246	mp-541785	GePdS ₃	C2/m	1.38	1.07	-	3.25 (1.73)	-	*
247	mp-1205339	Ge(SeO ₃) ₂	P2 ₁ /c	3.67	-	-	-	-	*
248	mp-1204060	Ge(SeO ₃) ₂	Pa $\bar{3}$	2.82	2.69	-	4.59 (2.73)	-	*
249	mp-554142	Ge(TeO ₃) ₂	P2 ₁ /c	3.79	2.64	-	-	-	*
250	mp-9755	HfGeO ₄	I4 ₁ /a	4.12	3.60	6.06 (4.17)	6.39 (4.06)	-	*
251	mp-687090	Hf(MoO ₄) ₂	P $\bar{3}1$ c	3.28	-	-	-	-	*
252	mp-22734	HfPbO ₃	Pbam	2.72	2.70	-	4.58 (2.72)	3.50 ¹²⁰	*
253	mp-22147	HfPbS ₃	Pnma	1.46	1.23	-	2.84 (1.43)	-	*
254	mp-7787	HfSO	P2 ₁ 3	2.89	1.98	3.95 (2.87)	4.78 (2.87)	4.50 ¹²⁰	*
255	mp-4609	HfSiO ₄	I4 ₁ /amd	5.30	4.62	5.45	8.06 (5.30)	-	*
256	mp-8725	HfSnS ₃	Pnma	1.22	1.17	1.17	2.58 (1.24)	1.60 ¹²¹	*
257	mp-18352	HfTe ₃ O ₈	Ia $\bar{3}$	3.84	2.94	-	6.10 (3.85)	-	
258	mp-1204711	Hf(WO ₄) ₂	P2 ₁ 3	3.92	3.29	-	6.06 (3.82)	-	
259	mp-5348	MgCO ₃	R $\bar{3}$ c	4.97	5.00	7.15 (5.22)	7.59 (4.96)	-	*
260	mp-504578	MgCrO ₄	C2/m	2.37	2.52	-	4.08 (2.35)	-	
261	mp-19120	MgCrO ₄	Cmcm	2.47	2.58	2.52 (2.23)	4.16 (2.41)	-	
262	mp-4575	MgGeO ₃	Pbca	2.90	3.06	-	4.73 (2.83)	-	*
263	mp-3051	Mg ₂ GeO ₄	Pnma	3.40	3.38	-	5.43 (3.35)	-	
264	mp-3904	Mg ₂ GeO ₄	Fd $\bar{3}$ m	3.07	2.85	5.22 (3.28)	4.98 (3.01)	-	
265	mp-27295	Mg ₁₄ Ge ₅ O ₂₄	Pbam	3.45	3.53	-	5.48 (3.39)	-	*
266	mp-17441	Mg ₂ GeS ₄	Pnma	2.31	2.31	-	3.99 (2.29)	-	*
267	mp-1192564	Mg ₂ GeSe ₄	Pnma	1.42	-	-	-	2.02 ¹⁰³	*
268	mp-19047	MgMoO ₄	C2/m	3.79	3.11	-	5.78 (3.61)	-	*
269	mp-27604	MgMo ₂ O ₇	P2 ₁ /c	3.67	3.08	-	5.64 (3.51)	-	*
270	mp-7572	MgSO ₄	Cmcm	5.49	5.06	6.05	8.30 (5.48)	-	
271	mp-1020122	MgS ₂ O ₇	P $\bar{1}$	5.52	-	8.05 (5.96)	-	-	
272	mp-12271	MgSeO ₃	Pnma	4.01	3.62	4.15	6.32 (4.01)	-	
273	mp-560670	MgSeO ₄	Pnma	3.13	-	4.78 (3.37)	-	-	
274	mp-16771	MgSe ₂ O ₅	Pbcn	3.03	3.18	3.10	4.98 (3.02)	-	
275	mp-556940	MgSiO ₃	Pbca	3.88	4.78	-	7.21 (4.67)	-	*
276	mp-2895	Mg ₂ SiO ₄	Pnma	4.64	4.42	-	7.18 (4.65)	-	*
277	mp-28663	Mg ₁₄ Si ₅ O ₂₄	Pbam	4.68	-	-	-	-	

278	mp-1193963	Mg ₂ SiS ₄	Pnma	2.97	2.88	-	4.91 (2.97)	-	
279	mp-1192582	Mg ₂ SiSe ₄	Pnma	2.13	2.01	-	3.79 (2.13)	-	
280	mp-5746	MgTe ₂ O ₅	Pbcn	2.37	2.90	-	4.13 (2.38)	-	*
281	mp-769077	Mg ₂ Te ₃ O ₈	C2/c	3.48	2.69	-	5.58 (3.46)	-	*
282	mp-3118	Mg ₃ TeO ₆	R $\bar{3}$	2.91	3.13	4.30 (3.11)	4.81 (2.89)	-	*
283	mp-3771	MgTiO ₃	R $\bar{3}$	3.50	3.36	4.02 (3.52)	6.07 (3.83)	-	*
284	mp-28232	MgTi ₂ O ₅	Cmcm	2.72	3.15	3.22 (2.73)	5.25 (3.22)	-	*
285	mp-18875	MgWO ₄	P2/c	3.68	3.17	4.18 (0.66)	5.42 (3.34)	-	*
286	mp-25082	Mo(CO) ₆	Pnma	3.15	2.48	-	5.27 (3.23)	-	*
287	mp-22169	MoPbO ₄	I4 ₁ /a	2.90	2.32	-	4.64 (2.76)	-	*
288	mp-21138	MoPb ₂ O ₅	C2/m	2.93	2.41	-	4.78 (2.87)	-	*
289	mp-652366	MoPb ₅ O ₈	P2 ₁ /c	2.40	-	-	-	-	*
290	mp-565836	MoSO ₆	C2/c	3.08	-	-	4.88 (2.94)	-	*
291	mp-640748	Os(CO) ₄	P2 ₁ /c	2.92	-	-	-	-	*
292	mp-679947	Os(CO) ₄	P $\bar{1}$	2.65	-	-	-	-	*
293	mp-28636	Os ₂ (CO) ₇	C2/c	2.00	-	-	-	-	*
294	mp-680248	Os ₅ (CO) ₁₆	P3 ₁ 21	1.99	-	-	-	-	*
295	mp-647725	Os ₅ C ₁₇ O ₁₆	P $\bar{1}$	2.02	-	-	-	-	*
296	mp-680286	Os ₅ (CO) ₁₉	P $\bar{1}$	2.03	-	-	-	-	*
297	mp-648157	Os ₆ C ₁₉ O ₂₀	Pnma	1.77	-	-	-	-	*
298	mp-19893	PbCO ₃	Pnma	3.33	-	4.87 (3.42)	-	-	
299	mp-22747	Pb(CO ₂) ₂	P $\bar{1}$	2.75	3.11	3.87 (2.86)	4.68 (2.79)	-	*
300	mp-1179835	Pb(CO) ₄	I4 ₁ /amd	3.02	2.72	-	4.98 (3.01)	-	*
301	mp-505702	Pb ₂ CO ₄	P2 ₁ 2 ₁ 2 ₁	3.41	2.99	-	5.53 (3.43)	-	*
302	mp-21190	PbSO ₃	P2 ₁ /m	3.24	3.13	5.17 (3.48)	5.25 (3.21)	-	
303	mp-3472	PbSO ₄	Pnma	4.00	3.41	-	6.30 (4.00)	-	
304	mp-21904	PbS ₂ O ₃	Pbca	3.47	-	-	5.70 (3.55)	-	*
305	mp-21497	Pb ₂ SO ₅	C2/m	3.13	3.02	3.22	5.11 (3.11)	-	
306	mp-22023	Pb ₃ SO ₆	P2 ₁ /m	2.94	2.42	-	4.89 (2.95)	-	
307	mp-505603	Pb ₅ SO ₈	P2 ₁ /c	2.45	-	-	-	-	*
308	mp-20716	PbSeO ₃	P2 ₁ /m	2.91	2.77	4.23 (3.05)	4.74 (2.84)	-	*
309	mp-22342	PbSeO ₄	P2 ₁ /c	3.19	2.51	-	4.46 (2.63)	-	
310	mp-662535	PbSe ₂ O ₅	P2 ₁ /c	3.10	2.91	-	5.24 (3.21)	-	*

311	mp-558163	Pb(SeO ₃) ₂	P2 ₁ /c	1.28	2.40	2.51 (1.36)	2.61 (1.26)	-	*
312	mp-22410	PbWO ₄	I4 ₁ /a	3.56	2.93	3.94 (3.30)	5.45 (3.37)	-	*
313	mp-22681	Pb ₂ WO ₅	C2/m	3.07	2.47	-	5.10 (3.10)	-	*
314	mp-28952	PdSO ₄	C2/c	1.06	1.77	1.13	3.66 (2.04)	-	*
315	mp-545482	PdSeO ₃	P2 ₁ /m	1.05	1.69	1.15	3.57 (1.97)	-	*
316	mp-561490	PdSeO ₄	C2/c	1.19	1.71	1.29	3.77 (2.12)	-	*
317	mp-4649	PdSe ₂ O ₅	C2/c	1.00	-	0.90	-	-	*
318	mp-29332	Pt(PbO ₂) ₂	Pbam	0.52	1.11	-	1.83 (0.68)	-	*
319	mp-652407	Ru(CO) ₄	P2 ₁ /c	2.59	-	-	-	-	*
320	mp-21723	SiPbO ₃	P2/c	3.16	-	-	-	-	*
321	mp-555786	Si(PbO ₂) ₂	C2/c	2.52	-	-	-	-	*
322	mp-21767	Si ₂ Pb ₃ O ₇	R $\bar{3}$ c	2.63	3.01	-	4.48 (2.64)	-	*
323	mp-1198381	Si ₃ Pb ₁₁ O ₁₇	P $\bar{1}$	2.03	-	-	-	-	
324	mp-504564	Si(PbS ₂) ₂	P2 ₁ /c	2.03	1.66	-	3.89 (2.21)	-	*
325	mp-27532	Si(PbSe ₂) ₂	P2 ₁ /c	1.82	1.26	-	3.23 (1.72)	-	*
326	mp-542769	Sn(CO ₂) ₂	C2/c	2.61	2.50	-	4.48 (2.65)	-	*
327	mp-5045	SnGeS ₃	P2 ₁ /c	1.61	1.62	2.07 (1.29)	2.89 (1.47)	2.23 ¹²²	*
328	mp-504543	SnPbO ₃	Fd $\bar{3}$ m	0.00	-	-	metal	3.26 ¹²³	
329	-	Sn(PbO ₂) ₂	Pbam	-	1.53	-	-	-	
330	mp-542967	SnSO ₄	Pnma	4.13	3.61	4.06	6.24 (3.95)	-	*
331	mp-31004	Sn(SO ₂) ₂	P2 ₁ /c	2.68	3.22	-	4.50 (2.66)	-	*
332	mp-28025	Sn ₂ SO ₅	P $\bar{4}$ 2 ₁ c	3.51	3.15	-	5.58 (3.46)	-	*
333	mp-555682	Sn(SeO ₃) ₂	P2 ₁ /c	3.08	2.09	-	4.37 (2.57)	-	*
334	mp-556672	Sn(SeO ₃) ₃	Pa $\bar{3}$	2.59	2.56	2.88	3.72 (2.08)	-	*
335	mp-12231	SnTe ₃ O ₈	Ia $\bar{3}$	2.93	2.62	3.34	4.41 (2.59)	-	
336	mp-17700	SnWO ₄	Pnna	0.92	2.66	-	3.09 (1.61)	-	*
337	mp-557633	Sn ₂ WO ₅	P2 ₁ /c	2.41	-	-	-	-	*
338	mp-556980	Sn ₃ WO ₆	C2/c	2.20	-	-	3.72 (2.08)	-	*
339	mp-3822	SrCO ₃	Pnma	4.43	4.36	-	6.90 (4.44)	-	*
340	mp-510607	SrCrO ₄	P2 ₁ /c	2.85	2.14	2.66	2.86 (1.44)	-	*
341	mp-557093	SrCr ₂ O ₇	P4 ₂ /nmc	2.48	-	-	-	-	*
342	mp-17464	SrGeO ₃	C2/c	3.39	-	5.54 (3.42)	5.39 (3.32)	-	*
343	mp-9380	SrGe ₄ O ₉	P321	3.07	-	-	4.97 (3.01)	-	*

344	mp-4578	Sr ₂ GeS ₄	P2 ₁ /m	2.33	2.32	2.21	3.99 (2.28)	-	*
345	mp-3378	SrHfO ₃	Pnma	4.17	3.88	4.28	6.53 (4.17)	-	
346	mp-1208643	SrHfS ₃	Pnma	1.49	-	-	2.93 (1.50)	2.18 ⁹⁶	
347	mp-18834	SrMoO ₄	I4 ₁ /a	3.81	3.29	4.27 (3.70)	5.90 (3.70)	-	*
348	mp-20489	SrPbO ₃	Pnma	0.80	1.25	0.85	1.98 (0.79)	1.80 ¹²⁴	*
349	mp-20944	Sr ₂ PbO ₄	Pbam	1.40	1.55	2.47 (1.43)	2.81 (1.40)	-	
350	mp-29775	Sr ₄ PdO ₆	R $\bar{3}$ c	1.58	1.84	1.80 (1.60)	3.34 (1.80)	-	
351	mp-4598	Sr ₄ PtO ₆	R $\bar{3}$ c	2.21	2.40	2.52 (2.22)	4.20 (2.43)	-	*
352	mp-5285	SrSO ₄	Pnma	5.91	5.41	6.52	8.86 (5.90)	-	*
353	mp-3395	SrSeO ₃	P2 ₁ /m	3.71	3.71	5.05 (3.74)	5.91 (3.70)	-	*
354	mp-555098	SrSeO ₃	Pnma	3.86	3.64	3.93	6.09 (3.84)	-	*
355	mp-4092	SrSeO ₄	P2 ₁ /c	3.51	3.66	5.16 (3.75)	5.31 (3.26)	-	*
356	mp-28346	SrSe ₂ O ₅	P $\bar{1}$	3.28	-	-	5.33 (3.28)	-	*
357	mp-3978	SrSiO ₃	C2/c	4.61	4.44	4.84	7.13 (4.62)	-	*
358	mp-18510	Sr ₂ SiO ₄	P2 ₁ /c	4.47	4.17	4.97	6.22 (3.93)	-	*
359	mp-5487	Sr ₃ SiO ₅	P4/ncc	3.76	3.74	6.02 (4.23)	6.01 (3.78)	-	
360	mp-1104926	Sr ₂ SiS ₄	P2 ₁ /m	2.90	2.53	-	4.85 (2.92)	-	
361	mp-2879	SrSnO ₃	Pnma	1.74	1.52	-	2.84 (1.43)	3.93 ¹²⁵	*
362	mp-1194203	Sr ₂ SnO ₄	Pccn	2.68	2.38	-	4.48 (2.65)	-	
363	mp-17743	Sr ₃ Sn ₂ O ₇	Cmcm	2.16	-	-	3.29 (1.76)	-	
364	mp-1179320	SrTeO ₃	C2/c	3.42	-	-	-	-	*
365	mp-4274	SrTeO ₄	Pbcn	2.23	2.58	3.55 (2.32)	3.94 (2.24)	-	*
366	mp-3252	SrTe ₃ O ₈	P4 ₂ /m	2.25	2.06	2.35	3.85 (2.18)	-	*
367	mp-1200112	Sr ₃ TeO ₆	P $\bar{1}$	3.01	-	-	-	-	*
368	mp-30026	Sr ₃ Te ₄ O ₁₁	P $\bar{1}$	3.17	3.04	-	5.20 (3.18)	-	*
369	mp-706599	Sr ₆ Te ₆ O ₁₇	C2/c	1.78	-	-	-	-	
370	mp-5229	SrTiO ₃	Pm $\bar{3}$ m	1.783 eV	2.35	2.30 (1.81)	4.00 (2.29)	-	*
371	mp-5532	Sr ₂ TiO ₄	I4/mmm	1.91	2.44	-	4.21 (2.45)	-	
372	mp-3349	Sr ₃ Ti ₂ O ₇	I4/mmm	1.84	-	1.89	4.12 (2.38)	-	
373	mp-31213	Sr ₄ Ti ₃ O ₁₀	I4/mmm	1.80	-	2.32 (1.84)	4.07 (2.34)	-	
374	mp-19163	SrWO ₄	I4 ₁ /a	4.66	3.47	-	6.87 (4.42)	-	*
375	mp-772676	Sr ₂ WO ₅	Pnma	3.19	-	-	-	-	
376	mp-5637	SrZnO ₂	Pnma	2.08	-	2.39	-	-	*

377	mp-1190981	Sr ₂ ZnS ₃	Pnma	2.42	2.31	-	4.24 (2.47)	-	
378	mp-4387	SrZrO ₃	Pnma	3.62	-	-	-	-	*
379	mp-27690	Sr ₃ Zr ₂ O ₇	I4/mmm	3.10	3.02	-	-	-	
380	mp-5193	SrZrS ₃	Pnma	1.19	1.35	1.24	2.51 (1.18)	2.05 ¹²⁶	*
381	mp-558760	SrZrS ₃	Pnma	0.55	-	-	1.68 (0.57)	1.52 ¹²⁶	*
382	mp-19453	Te ₂ MoO ₇	P2 ₁ /c	2.81	2.16	-	4.65 (2.77)	-	
383	mp-543039	TePbO ₃	C2/c	3.04	-	-	-	-	*
384	mp-1105700	TePb ₂ O ₅	C2/c	2.09	2.00	-	3.62 (2.01)	-	*
385	mp-1201764	TePb ₅ O ₈	P2 ₁ /c	2.16	-	-	-	-	*
386	mp-21922	Te ₃ (PbO ₄) ₂	Cmcm	3.00	-	-	-	-	*
387	mp-1203659	Te ₅ PbO ₁₁	C2/c	3.10	-	-	-	-	*
388	mp-29320	Te ₃ SeO ₈	P $\bar{1}$	2.62	2.64	4.38 (2.79)	4.47 (2.64)	-	*
389	mp-1008680	TiGePt	F $\bar{4}3m$	0.89	0.50	0.94	2.16 (0.93)	0.90 ¹²⁷	*
390	mp-504427	Ti ₃ PbO ₇	P2 ₁ /m	1.98	2.52	-	4.08 (2.35)	-	
391	mp-554944	TiSO ₅	Pnma	2.11	2.84	-	4.12 (2.38)	-	
392	mp-29260	Ti(SeO ₃) ₂	P2 ₁ /c	2.45	2.58	2.46	4.73 (2.83)	-	*
393	mp-18288	Ti(SnO ₂) ₂	P4 ₂ /mbc	1.08	2.26	-	2.89 (1.47)	1.55 ¹²⁸	*
394	mp-30847	TiSnPt	F $\bar{4}3m$	0.80	0.43	0.83	1.78 (0.65)	-	*
395	mp-5214	TiTe ₃ O ₈	Ia $\bar{3}$	2.73	2.80	2.73	5.05 (3.07)	-	*
396	mp-14142	TiZnO ₃	R $\bar{3}$	2.98	3.05	3.05	5.64 (3.50)	-	
397	mp-542737	TiZn ₂ O ₄	P4 ₁ 22	2.31	2.91	-	5.09 (3.10)	-	*
398	mp-541695	W(CO) ₆	Pnma	2.98	2.77	-	5.09 (3.10)	-	
399	mp-1201710	WS ₂ O ₉	P2 ₁ /c	3.83	2.06	-	3.86 (2.19)	-	*
400	mp-9812	ZnCO ₃	R $\bar{3}c$	3.56	3.88	5.94 (3.87)	6.43 (4.09)	-	
401	mp-559437	Zn(CO ₂) ₂	P2 ₁ /c	3.20	-	4.34 (3.27)	-	-	
402	mp-8285	ZnGeO ₃	R $\bar{3}$	2.11	2.22	4.06 (2.37)	4.50 (2.66)	-	*
403	mp-5909	Zn ₂ GeO ₄	R $\bar{3}$	1.97	-	-	4.26 (2.48)	-	*
404	mp-27843	Zn ₂ Ge ₃ O ₈	P4 ₃ 22	2.34	2.50	-	4.50 (2.66)	-	
405	mp-16882	ZnMoO ₄	P $\bar{1}$	3.54	3.08	-	5.85 (3.66)	-	*
406	mp-29461	Zn ₃ Mo ₂ O ₉	P2 ₁ /m	3.16	3.05	3.13 (3.01)	5.39 (3.32)	-	*
407	mp-5126	ZnSO ₄	Pnma	3.82	4.09	4.25	6.92 (4.46)	-	*
408	mp-30986	Zn ₃ S ₂ O ₉	P2 ₁ /m	3.37	4.05	-	-	-	*
409	mp-5338	ZnSeO ₃	Pbca	3.91	3.73	4.13	6.69 (4.29)	-	*

410	mp-4682	ZnSeO ₃	Pnma	3.45	3.59	3.66	5.94 (3.73)	-	*
411	mp-18373	ZnSe ₂ O ₅	Pbcn	3.04	3.38	-	4.92 (2.97)	-	*
412	mp-619034	ZnSiO ₃	Pbca	3.39	-	-	6.39 (4.06)	-	*
413	mp-562182	ZnSiO ₃	C2/c	3.48	-	5.36 (3.67)	6.46 (4.12)	-	*
414	mp-3789	Zn ₂ SiO ₄	R $\bar{3}$	2.75	-	-	5.56 (3.45)	-	*
415	mp-16819	ZnTeO ₃	Pbca	3.47	3.27	-	5.76 (3.59)	-	*
416	mp-560198	ZnTe ₆ O ₁₃	R $\bar{3}$	2.97	2.57	-	4.95 (3.00)	-	*
417	mp-3502	Zn ₂ Te ₃ O ₈	C2/c	3.30	3.18	-	5.47 (3.38)	-	*
418	mp-13199	Zn ₃ TeO ₆	C2/c	1.06	-	-	3.25 (1.73)	-	*
419	mp-18918	ZnWO ₄	P2/c	3.22	2.81	-	5.05 (3.07)	-	*
420	mp-8042	ZrGeO ₄	I4 ₁ /a	3.73	3.63	4.84 (3.90)	5.97 (3.75)	-	*
421	mp-27888	Zr ₃ GeO ₈	I $\bar{4}$ 2m	3.90	3.47	4.78 (4.14)	6.14 (3.88)	-	
422	mp-510456	Zr(MoO ₄) ₂	P $\bar{3}$ m1	3.12	3.05	3.77 (3.17)	5.02 (3.05)	-	*
423	mp-542903	ZrPbO ₃	Pbam	2.78	2.66	-	4.65 (2.77)	-	*
424	mp-20244	ZrPbS ₃	Pnma	1.25	insulator	1.27	-	-	*
425	mp-3519	ZrSO	P2 ₁ 3	2.43	1.55	2.93 (2.45)	4.17 (2.41)	4.30 ¹²⁰	
426	mp-4325	Zr(SO ₄) ₂	Pnma	3.56	-	3.81	5.73 (3.57)	-	*
427	mp-4820	ZrSiO ₄	I4 ₁ /amd	4.45	3.95	5.19 (4.70)	6.93 (4.46)	-	*
428	mp-17324	ZrSnS ₃	Pnma	1.00	0.90	-	2.34 (1.06)	1.50 ¹²¹	*
429	mp-4759	ZrTe ₃ O ₈	Ia $\bar{3}$	3.67	2.79	-	5.85 (3.66)	-	
430	mp-1207388	Zr ₃ TiO ₈	I $\bar{4}$ 2m	3.29	-	-	-	-	
431	mp-18778	Zr(WO ₄) ₂	P2 ₁ 3	3.61	3.30	-	5.70 (3.55)	3.80 ¹²⁹	

Table 4. The potentially viable higher-order host materials. All band gaps are reported in eV. Phases reported in the JARVIS-DFT database for which both standard OPT and hybrid OPT-mBJ calculations were performed are listed with the OPT-mBJ listed first, followed by the smaller OPT band gap in parentheses. Where the OPT-mBJ-computed band gap was found to be unrealistically small, compared to the basic OPT-calculated one, only the OPT-computed band gap is listed. Where multiple AFLOW repository entries were found to exist for the same phase of a compound, the average of each computed band gap size is listed. Literature band gaps listed in bold correspond to those experimentally-derived, while those not bolded correspond to reported, alternatively calculated band gap widths, many of which are seen to agree with the database DFT-calculations. The presence of * in the SC column denotes a known single-crystal synthesis method for that particular phase. (-) in any cell corresponds to uncalculated and unreported values for that particular phase, respectively. Grayed text indicates materials where the band gap is considered to be near enough to that of elemental Si to be potentially viable.

				Band Gap (eV)					
Entry #	Materials ID	Formula	Space Group	Materials Project	AFLOW-ML	Jarvis OPT-mBJ (OPT)	AFLOW $E_{gfit}(E_{gap})$	Literature	SC
432	mp-556458	BaCa(CO ₃) ₂	P321	4.13	4.46	-	6.47 (4.13)	-	
433	mp-6568	BaCa(CO ₃) ₂	P2 ₁ /m	4.69	4.44	-	-	-	
434	mp-19403	Ba ₂ CaMoO ₆	Fm $\bar{3}$ m	2.26	2.29	2.73	3.77 (2.12)	-	
435	mp-17380	Ba ₂ Ca(PdO ₂) ₃	Fmmm	1.29	1.48	-	3.70 (2.07)	-	*
436	mp-18216	BaCa ₂ (SiO ₃) ₃	P $\bar{1}$	4.57	4.46	-	7.06 (4.56)	-	
437	mp-550685	Ba ₂ CaTeO ₆	Fm $\bar{3}$ m	3.00	2.75	4.29 (3.25)	4.95 (3.00)	-	
438	mp-18977	Ba ₂ CaWO ₆	Fm $\bar{3}$ m	3.18	3.03	0.57	4.76 (2.86)	-	
439	mp-1192417	BaGePbO ₄	P2 ₁ 2 ₁ 2 ₁	3.45	-	-	-	-	*
440	mp-1019548	BaGe(S ₂ O ₇) ₃	P2 ₁ 2 ₁ 2 ₁	3.95	-	-	-	-	*
441	mp-570803	Ba ₂ Ge(TeSe) ₂	P2 ₁ /m	0.84	1.03	-	2.01 (0.82)	1.00 ¹³⁰	*
442	mp-1194160	BaHf(SiO ₃) ₃	P6c2	4.68	4.45	-	7.24 (4.70)	-	
443	mp-1205395	BaMg(CO ₃) ₂	R $\bar{3}$ c	4.21	-	6.22 (4.24)	-	-	*
444	mp-1190545	Ba ₂ MgGe ₂ O ₇	P $\bar{4}$ 2 ₁ m	3.61	3.40	-	5.71 (3.56)	-	*
445	mp-1019549	BaMg ₂ Si ₂ O ₇	C2/c	4.56	-	-	-	-	
446	mp-9338	Ba ₂ MgSi ₂ O ₇	P $\bar{4}$ 2 ₁ m	4.46	4.47	4.70	6.93 (4.46)	-	*
447	mp-556703	Ba ₃ Mg(SiO ₄) ₂	P $\bar{3}$	4.69	3.88	-	7.25 (4.70)	-	
448	mp-18986	Ba ₂ MgWO ₆	Fm $\bar{3}$ m	3.23	2.97	-	4.84 (2.91)	-	*
449	mp-556779	BaMoSeO ₆	P2 ₁ /c	3.07	2.78	-	4.94 (2.99)	-	*

450	mp-1205352	BaPd(SeO ₃) ₂	C2/c	1.53	-	-	-	-	2.15 ¹³¹	*
451	mp-1201400	BaSi(S ₂ O ₇) ₃	Pbca	5.29	-	-	-	-	-	*
452	mp-18502	BaSi ₃ SnO ₉	P $\bar{6}$ c2	3.72	3.37	3.93	5.44 (3.36)	-	-	
453	mp-540635	BaSn(GeO ₃) ₃	P $\bar{6}$ c2	2.77	2.58	2.87	4.55 (2.70)	-	-	
454	mp-13356	Ba ₂ SrTeO ₆	R $\bar{3}$	3.13	2.98	4.42 (3.43)	5.13 (3.12)	-	-	
455	mp-18764	Ba ₂ SrWO ₆	C2/m	3.26	-	3.85 (0.59)	-	-	-	
456	mp-558894	Ba ₄ Ti ₂ PtO ₁₀	Cmce	2.00	-	-	-	-	-	*
457	mp-1198551	BaTi(S ₂ O ₇) ₃	P2 ₁ /c	2.72	-	-	-	-	-	*
458	mp-6661	BaTi(SiO ₃) ₃	P $\bar{6}$ c2	3.07	3.85	-	5.70 (3.55)	-	-	
459	mp-1190949	Ba ₂ ZnGe ₂ O ₇	P $\bar{4}$ 2 ₁ m	3.10	3.19	-	5.45 (3.37)	-	-	*
460	mp-548469	BaZnSO	Cmcm	2.24	2.04	2.42	4.17 (2.42)	3.90 ¹³²	*	
461	mp-1205399	BaZn(SeO ₃) ₂	P2 ₁ /c	3.77	-	-	-	-	-	*
462	mp-558629	Ba ₂ ZnSi ₂ O ₇	C2/c	4.00	4.12	-	6.67 (4.28)	-	-	*
463	mp-1078410	Ba ₂ ZnTeO ₆	Fm $\bar{3}$ m	0.43	-	-	-	3.00 ¹³³	-	
464	mp-548615	Ba ₂ ZnWO ₆	Fm $\bar{3}$ m	3.41	2.87	-	4.94 (2.99)	-	-	*
465	mp-1078457	Ba ₂ ZrTiO ₆	Fm $\bar{3}$ m	2.21	-	-	-	-	-	
466	mp-1202124	Ba ₆ Zr(Zn ₃ S ₇) ₂	I4/mcm	1.76	-	-	-	-	-	*
467	mp-15003	Ca ₃ HfSi ₂ O ₉	P2 ₁ /c	4.68	4.37	-	7.23 (4.68)	-	-	
468	mp-6459	CaMg(CO ₃) ₂	R $\bar{3}$	5.01	4.77	5.17	7.66 (5.00)	-	-	
469	mp-6524	CaMg ₃ (CO ₃) ₄	R32	4.83	4.71	-	7.40 (4.81)	-	-	
470	mp-558362	CaMgGeO ₄	Pnma	3.62	-	5.85 (3.75)	-	-	-	*
471	mp-554094	CaMg ₂ (SO ₄) ₃	P6 ₃ /m	5.76	5.33	-	8.50 (5.63)	-	-	*
472	mp-6493	CaMgSiO ₄	Pnma	4.63	-	5.14	-	-	-	
473	mp-562517	CaMg(SiO ₃) ₂	C2/c	4.66	-	7.36 (4.89)	7.60 (4.96)	-	-	
474	mp-541026	CaMg ₃ Si ₃ O ₁₀	P $\bar{1}$	3.41	-	-	-	-	-	
475	mp-6094	Ca ₂ MgSi ₂ O ₇	P $\bar{4}$ 2 ₁ m	4.47	4.42	6.90 (4.79)	6.93 (4.46)	-	-	*
476	mp-558079	Ca ₃ Mg(SiO ₄) ₂	P2 ₁ /c	3.82	-	-	-	-	-	*
477	mp-19324	Ca ₂ MgWO ₆	P2 ₁ /c	3.73	3.13	-	5.54 (3.43)	-	-	
478	mp-6796	Ca ₅ Si ₂ CO ₁₁	P2 ₁ /c	4.60	-	-	-	-	-	
479	mp-6753	Ca ₅ Si ₂ C ₂ O ₁₃	P2 ₁ /c	4.79	-	-	-	-	-	
480	mp-504590	Ca ₂ Si ₃ PbO ₉	P $\bar{1}$	4.35	3.61	-	6.79 (4.36)	-	-	
481	mp-6607	Ca ₅ Si ₂ SO ₁₂	Pnma	4.44	-	-	6.91 (4.45)	-	-	
482	mp-555508	Ca ₁₁ Si ₄ SO ₁₈	I $\bar{4}$ m2	3.53	3.64	-	5.64 (3.51)	-	-	

483	mp-6809	CaSiSnO ₅	C2/c	3.22	-	5.05 (3.51)	-	-	
484	mp-15095	Ca ₃ Si ₂ SnO ₉	P2 ₁ /c	3.44	-	3.66	5.09 (3.10)	-	
485	mp-559128	CaTeCO ₅	Pbca	3.85	3.35	-	6.10 (3.85)	-	
486	mp-1205333	CaTiGeO ₅	C2/c	2.72	insulator	-	-	-	*
487	mp-1105917	CaTi ₄ (PdO ₄) ₃	I $\bar{m}\bar{3}$	0.45	-	-	-	2.94-3.20 ¹³⁴	
488	mp-6109	CaTiSiO ₅	P2 ₁ /c	2.96	-	2.96	3.94 (2.24)	-	*
489	mp-9413	Ca ₂ TiSiO ₆	Fm $\bar{3}$ m	2.36	3.25	2.96	4.64 (2.76)	-	
490	mp-1078391	CaZn(CO ₃) ₂	R $\bar{3}$	3.97	-	-	-	-	
491	mp-12326	CaZn(GeO ₃) ₂	C2/c	2.47	2.65	-	4.56 (2.70)	-	*
492	mp-18596	Ca ₂ ZnGe ₂ O ₇	P $\bar{4}2_1$ m	3.05	3.12	4.76 (3.13)	5.32 (3.27)	-	*
493	mp-6693	CaZn(SiO ₃) ₂	C2/c	4.06	4.29	4.40	6.97 (4.49)	-	*
494	mp-554905	CaZnSi ₃ O ₈	P $\bar{1}$	4.09	-	-	6.83 (4.39)	-	*
495	mp-6227	Ca ₂ ZnSi ₂ O ₇	P $\bar{4}2_1$ m	4.06	4.23	-	6.76 (4.34)	-	*
496	mp-14778	Ca ₃ Zn ₃ (TeO ₆) ₂	Ia $\bar{3}$ d	2.13	2.38	-	4.23 (2.46)	-	
497	mp-555961	Ca ₃ Zn ₃ (TeO ₆) ₂	I4 ₁ 32	1.85	2.39	-	3.80 (2.15)	-	
498	mp-644295	CaZrGeO ₅	P $\bar{1}$	3.90	3.01	-	3.13 (1.64)	-	
499	mp-560339	Ca ₂ Zr(SiO ₃) ₄	P2 ₁ /m	4.85	4.60	-	7.45 (4.85)	-	*
500	mp-15004	Ca ₃ ZrSi ₂ O ₉	P2 ₁ /c	4.46	4.40	-	6.92 (4.46)	-	
501	mp-667369	Ca ₂ Zr ₅ Ti ₂ O ₁₆	Pbca	3.09	-	-	-	-	
502	mp-647840	Fe ₂ C ₈ SO ₁₀	P2 ₁ /c	2.44	-	-	-	-	*
503	mp-652326	Fe ₃ C ₉ S ₂ O ₉	P $\bar{1}$	1.92	-	-	3.81 (2.15)	-	*
504	mp-654299	Fe ₃ C ₉ (SO ₅) ₂	P $\bar{1}$	2.17	-	-	3.95 (2.25)	-	
505	mp-648633	Fe ₃ C ₁₀ SO ₁₀	P2 ₁ /c	2.39	-	-	-	-	
506	mp-653596	Fe ₄ Si(CO) ₁₆	P2 ₁ /c	2.62	-	-	-	-	*
507	mp-653267	Fe ₆ Sn ₂ (CO) ₂₃	P $\bar{1}$	2.13	-	-	-	-	
508	mp-652337	Fe ₃ Te ₂ (CO) ₉	P $\bar{1}$	1.72	-	-	3.43 (1.87)	-	*
509	mp-1197913	GePb(S ₂ O ₇) ₃	P $\bar{1}$	3.96	-	-	-	-	*
510	mp-1198509	GePb ₂ (SeO ₃) ₄	P2 ₁ /c	3.33	-	-	5.36 (3.30)	4.10 ¹³⁵	*
511	mp-20056	MgPb ₂ WO ₆	Fm $\bar{3}$ m	2.86	2.63	-	4.40 (2.59)	-	*
512	mp-20216	MgPb ₂ WO ₆	Pnma	2.86	-	-	-	-	
513	mp-1210722	MgTeMoO ₆	P2 ₁ 2 ₁ 2	3.15	-	-	-	-	*
514	mp-21309	MgTe(PbO ₃) ₂	Fm $\bar{3}$ m	2.27	2.10	-	3.94 (2.24)	-	
515	mp-1196979	MoPbSeO ₆	P $\bar{1}$	2.33	-	-	3.67 (2.04)	-	*

516	mp-1204412	Mo ₂ PbSe ₂ O ₁₁	P $\bar{1}$	2.50	-	-	4.13 (2.39)	-	*
517	mp-1196196	NiRu ₅ C ₁₇ O ₁₆	P $\bar{1}$	1.92	-	-	-	-	
518	mp-662792	Os ₂ C ₆ SO ₆	P $\bar{1}$	2.00	-	-	-	-	
519	mp-648289	Os ₃ C ₈ SO ₈	P2 ₁ /c	1.76	-	-	-	-	*
520	mp-679948	Os ₃ C ₈ (SO ₄) ₂	P2 ₁ /c	0.00	-	-	-	-	*
521	mp-608431	Os ₃ C ₉ S ₂ O ₉	P $\bar{1}$	2.51	-	-	-	-	*
522	mp-621927	Os ₃ C ₁₀ SO ₁₀	P $\bar{1}$	2.82	2.57	-	4.68 (2.80)	-	*
523	mp-649945	Os ₄ C ₁₃ SO ₁₃	P $\bar{1}$	1.96	-	-	-	-	*
524	mp-662796	Os ₄ C ₁₃ (SO ₆) ₂	P $\bar{1}$	1.90	-	-	-	-	*
525	mp-648263	Os ₄ C ₁₃ S ₂ O ₁₃	P2 ₁ /c	2.03	-	-	-	-	*
526	mp-648264	Os ₆ C ₁₇ S ₂ O ₁₇	P2 ₁ 2 ₁ 2 ₁	1.80	-	-	-	-	*
527	mp-662802	Os ₆ C ₁₉ SO ₁₉	P $\bar{1}$	1.71	-	-	-	-	*
528	mp-651026	Os ₂ C ₆ SeO ₆	P $\bar{1}$	1.85	-	-	-	-	*
529	mp-649754	Os ₃ C ₉ Se ₂ O ₉	P $\bar{1}$	2.39	-	-	-	-	*
530	mp-615529	Os ₂ Pt(CO) ₁₀	P $\bar{1}$	2.59	-	-	4.30 (2.51)	-	*
531	mp-1196932	Pb ₂ C(SO ₃) ₂	Pnma	2.80	-	-	4.59 (2.73)	-	
532	mp-650978	Ru ₅ C ₁₄ (SO ₇) ₂	P2 ₁ /c	1.76	-	-	-	-	*
533	mp-650984	Ru ₆ C ₁₇ S ₂ O ₁₇	P2 ₁ 2 ₁ 2 ₁	0.90	-	-	-	-	*
534	mp-650996	Ru ₇ C ₂₀ (SO ₁₀) ₂	P2 ₁ 2 ₁ 2 ₁	1.07	-	-	-	-	*
535	mp-629476	RuC ₃ SeO ₃	I4̄3m	2.19	-	-	-	-	*
536	mp-1203202	Ru ₃ C ₉ Se ₂ O ₉	P $\bar{1}$	2.24	-	-	-	-	*
537	mp-19116	Sr ₂ CaMoO ₆	P2 ₁ /c	2.55	-	-	-	-	
538	mp-11982	Sr ₂ CaTeO ₆	P2 ₁ /c	3.21	-	-	-	-	
539	mp-1192743	SrGePbO ₄	P2 ₁ 2 ₁ 2 ₁	3.49	-	-	-	-	*
540	mp-1020704	Sr ₂ Ge(S ₂ O ₇) ₄	P2 ₁ /c	3.43	-	-	-	-	*
541	mp-10341	SrGeTeO ₆	P312	2.96	2.70	-	4.90 (2.96)	-	
542	mp-972387	Sr ₂ MgGe ₂ O ₇	P4̄2 ₁ m	3.61	3.38	-	5.70 (3.55)	-	*
543	mp-1078539	Sr ₂ MgMoO ₆	I4/m	2.29	2.44	-	3.90 (2.21)	-	
544	mp-6064	Sr ₃ MgPtO ₆	R3̄c	2.66	2.29	-	4.98 (3.01)	-	
545	mp-6564	Sr ₂ MgSi ₂ O ₇	P4̄2 ₁ m	4.50	4.48	-	6.97 (4.49)	-	*
546	mp-554641	Sr ₃ Mg(SiO ₄) ₂	C2/c	4.69	-	-	-	-	
547	mp-1078995	Sr ₂ MgTeO ₆	C2/m	2.33	-	-	-	-	
548	mp-19420	Sr ₂ MgWO ₆	I4/m	3.43	3.04	-	5.05 (3.07)	-	

549	mp-1200408	SrMo ₂ Se ₂ O ₁₁	P $\bar{1}$	2.73	-	-	4.41 (2.59)	-	*
550	mp-556331	Sr ₄ Pt ₄ PbO ₁₁	P $\bar{1}$	0.57	1.54	-	2.20 (0.96)	-	*
551	mp-1020612	Sr ₂ Si(S ₂ O ₇) ₄	P2 ₁ /c	4.91	-	-	-	-	*
552	mp-559957	SrTiGeO ₅	P2 ₁ /c	2.84	2.79	-	-	-	
553	mp-559208	SrTiSi ₂ O ₇	Cmcm	3.61	3.71	3.73 (3.66)	6.62 (4.24)	-	
554	mp-558553	Sr ₄ Ti ₅ (Si ₂ O ₁₁) ₂	C2/m	1.94	-	-	-	-	
555	mp-17392	Sr ₂ ZnGe ₂ O ₇	P $\bar{4}$ 2 ₁ m	3.12	3.09	-	5.42 (3.34)	-	*
556	mp-1079971	Sr ₂ ZnMoO ₆	I4/m	2.38	2.31	-	4.01 (2.30)	-	
557	mp-6730	Sr ₃ ZnPtO ₆	R $\bar{3}$ c	2.56	2.27	2.65	4.93 (2.98)	-	*
558	mp-555691	SrZn(SeO ₃) ₂	P2 ₁ /c	4.33	3.62	-	6.75 (4.33)	-	*
559	mp-1191240	Sr ₂ ZnSi ₂ O ₇	P $\bar{4}$ 2 ₁ m	3.90	4.13	-	6.68 (4.28)	-	
560	mp-1079778	Sr ₂ ZnWO ₆	I4/m	3.53	-	-	-	-	
561	mp-1105272	Sr ₂ ZnWO ₆	P2 ₁ /c	3.51	-	-	-	-	
562	mp-17468	SrZrSi ₂ O ₇	P2 ₁ /c	4.71	-	-	-	-	
563	mp-555314	Sr ₇ Zr(Si ₂ O ₇) ₃	R $\bar{3}$	4.43	-	-	-	-	*
564	mp-1080028	Sr ₂ ZrTiO ₆	I4/m	2.51	-	-	-	-	
565	mp-651231	Te ₂ Ru ₄ (CO) ₁₁	Pccn	1.74	-	-	-	-	*
566	mp-651051	Te ₂ W ₃ (CO) ₁₅	P4 ₁ 2 ₁ 2	1.22	-	-	-	-	*
567	mp-1203799	TiPb(S ₂ O ₇) ₃	P2 ₁ /c	2.72	-	-	-	-	*
568	mp-558830	ZnTeMoO ₆	P2 ₁ 2 ₁ 2	3.09	2.78	3.70 (2.98)	4.98 (3.02)	-	*
569	mp-1103554	BaCa ₂ Mg(SiO ₄) ₂	P $\bar{3}$	4.97	4.46	-	7.63 (4.99)	-	
570	mp-1019558	BaSr ₂ Mg(SiO ₄) ₂	P $\bar{3}$ m1	4.76	-	6.89 (5.26)	-	-	
571	mp-17244	Ba ₂ ZnGe ₂ S ₆ O	P $\bar{4}$ 2 ₁ m	2.09	2.30	-	3.72 (2.08)	-	*
572	mp-543034	Ba ₃ Zn ₆ Si ₄ TeO ₂₀	C2/m	2.64	3.08	-	5.29 (3.24)	-	*
573	mp-1200437	Ca ₂ Zn ₃ Si ₃ PbO ₁₂	P2 ₁ /c	3.71	-	-	-	-	
574	mp-652318	CrFe ₂ C ₁₀ (Se ₂ O ₅) ₂	P2 ₁ /c	1.52	-	-	-	-	*
575	mp-651724	Fe ₂ Te ₂ Ru ₂ (CO) ₁₁	Pccn	1.70	-	-	-	-	*
576	mp-559754	Fe ₂ Te ₂ W(CO) ₁₀	P $\bar{1}$	1.93	-	-	-	-	*
577	mp-557864	Fe ₂ WC ₁₀ (SeO ₅) ₂	P $\bar{1}$	1.96	-	-	-	-	*
578	mp-558938	Zn ₄ SiTePbO ₁₀	Pnma	2.29	-	-	-	-	*
579	mp-683831	Fe ₃ MoC ₁₁ SeS ₃ O ₁₁	P2 ₁ /c	2.12	-	-	-	-	*
580	mp-624009	Fe ₂ TeWC ₁₀ SeO ₁₀	P $\bar{1}$	1.91	-	-	-	-	*

References

- (1) Kimble, H. J. The Quantum Internet. *Nature*. Nature Publishing Group June 19, 2008, pp 1023–1030. <https://doi.org/10.1038/nature07127>.
- (2) Awschalom, D. D.; Hanson, R.; Wrachtrup, J.; Zhou, B. B. Quantum Technologies with Optically Interfaced Solid-State Spins. *Nature Photonics*. Nature Publishing Group September 1, 2018, pp 516–527. <https://doi.org/10.1038/s41566-018-0232-2>.
- (3) Maze, J. R.; Stanwix, P. L.; Hodges, J. S.; Hong, S.; Taylor, J. M.; Cappellaro, P.; Jiang, L.; Dutt, M. V. G.; Togan, E.; Zibrov, A. S.; et al. Nanoscale Magnetic Sensing with an Individual Electronic Spin in Diamond. *Nature* **2008**, *455* (7213), 644–647. <https://doi.org/10.1038/nature07279>.
- (4) Awschalom, D. D.; Bassett, L. C.; Dzurak, A. S.; Hu, E. L.; Petta, J. R. Quantum Spintronics: Engineering and Manipulating Atom-like Spins in Semiconductors. *Science*. American Association for the Advancement of Science March 8, 2013, pp 1174–1179. <https://doi.org/10.1126/science.1231364>.
- (5) Rogers, L. J.; Jahnke, K. D.; Metsch, M. H.; Sipahigil, A.; Binder, J. M.; Teraji, T.; Sumiya, H.; Isoya, J.; Lukin, M. D.; Hemmer, P.; et al. All-Optical Initialization, Readout, and Coherent Preparation of Single Silicon-Vacancy Spins in Diamond. *Phys. Rev. Lett.* **2014**, *113* (26), 263602.
<https://doi.org/10.1103/PhysRevLett.113.263602>.
- (6) Rose, B. C.; Huang, D.; Zhang, Z. H.; Stevenson, P.; Tyryshkin, A. M.; Sangtawesin, S.; Srinivasan, S.; Loudin, L.; Markham, M. L.; Edmonds, A. M.; et al. Observation of an Environmentally Insensitive Solid-State Spin Defect in Diamond. *Science* (80-.). **2018**, *361* (6397), 60–63.
<https://doi.org/10.1126/science.aa0290>.
- (7) Bhaskar, M. K.; Sukachev, D. D.; Sipahigil, A.; Evans, R. E.; Burek, M. J.; Nguyen, C. T.; Rogers, L. J.; Siyushev, P.; Metsch, M. H.; Park, H.; et al. Quantum Nonlinear Optics with a Germanium-Vacancy Color Center in a Nanoscale Diamond Waveguide. *Phys. Rev. Lett.* **2017**, *118* (22), 223603.
<https://doi.org/10.1103/PhysRevLett.118.223603>.
- (8) Iwasaki, T.; Miyamoto, Y.; Taniguchi, T.; Siyushev, P.; Metsch, M. H.; Jelezko, F.; Hatano, M. Tin-Vacancy Quantum Emitters in Diamond. *Phys. Rev. Lett.* **2017**, *119* (25), 253601. <https://doi.org/10.1103/PhysRevLett.119.253601>.
- (9) Trusheim, M. E.; Wan, N. H.; Chen, K. C.; Ciccarino, C. J.; Flick, J.; Sundararaman, R.; Malladi, G.; Bersin, E.; Walsh, M.; Lienhard, B.; et al. Lead-Related Quantum Emitters in Diamond. *Phys. Rev. B* **2019**, *99* (7), 075430.
<https://doi.org/10.1103/PhysRevB.99.075430>.
- (10) Koehl, W. F.; Buckley, B. B.; Heremans, F. J.; Calusine, G.; Awschalom, D. D.

Room Temperature Coherent Control of Defect Spin Qubits in Silicon Carbide. *Nature* **2011**, *479* (7371), 84–87. <https://doi.org/10.1038/nature10562>.

- (11) Togan, E.; Chu, Y.; Trifonov, A. S.; Jiang, L.; Maze, J.; Childress, L.; Dutt, M. V. G.; Sørensen, A. S.; Hemmer, P. R.; Zibrov, A. S.; et al. Quantum Entanglement between an Optical Photon and a Solid-State Spin Qubit. *Nature* **2010**, *466* (7307), 730–734. <https://doi.org/10.1038/nature09256>.
- (12) Hensen, B.; Bernien, H.; Dreaú, A. E.; Reiserer, A.; Kalb, N.; Blok, M. S.; Ruitenberg, J.; Vermeulen, R. F. L.; Schouten, R. N.; Abellán, C.; et al. Loophole-Free Bell Inequality Violation Using Electron Spins Separated by 1.3 Kilometres. *Nature* **2015**, *526* (7575), 682–686. <https://doi.org/10.1038/nature15759>.
- (13) Taylor, J. M.; Cappellaro, P.; Childress, L.; Jiang, L.; Budker, D.; Hemmer, P. R.; Yacoby, A.; Walsworth, R.; Lukin, M. D. High-Sensitivity Diamond Magnetometer with Nanoscale Resolution. *Nat. Phys.* **2008**, *4* (10), 810–816. <https://doi.org/10.1038/nphys1075>.
- (14) Lovchinsky, I.; Sushkov, A. O.; Urbach, E.; De Leon, N. P.; Choi, S.; De Greve, K.; Evans, R.; Gertner, R.; Bersin, E.; Muller, C.; et al. Nuclear Magnetic Resonance Detection and Spectroscopy of Single Proteins Using Quantum Logic. *Science* (80-.). **2016**, *351* (6275), 836–841. <https://doi.org/10.1126/science.aad8022>.
- (15) Dolde, F.; Fedder, H.; Doherty, M. W.; Nöbauer, T.; Rempp, F.; Balasubramanian, G.; Wolf, T.; Reinhard, F.; Hollenberg, L. C. L.; Jelezko, F.; et al. Electric-Field Sensing Using Single Diamond Spins. *Nat. Phys.* **2011**, *7* (6), 459–463. <https://doi.org/10.1038/nphys1969>.
- (16) Kucsko, G.; Maurer, P. C.; Yao, N. Y.; Kubo, M.; Noh, H. J.; Lo, P. K.; Park, H.; Lukin, M. D. Nanometre-Scale Thermometry in a Living Cell. *Nature* **2013**, *500* (7460), 54–58. <https://doi.org/10.1038/nature12373>.
- (17) Fukami, M.; Yale, C. G.; Andrich, P.; Liu, X.; Heremans, F. J.; Nealey, P. F.; Awschalom, D. D. All-Optical Cryogenic Thermometry Based on NV Centers in Nanodiamonds. *Phys. Rev. Appl.* **2019**, *12* (1). <https://doi.org/10.1103/PhysRevApplied.12.014042>.
- (18) Glenn, D. R.; Bucher, D. B.; Lee, J.; Lukin, M. D.; Park, H.; Walsworth, R. L. High-Resolution Magnetic Resonance Spectroscopy Using a Solid-State Spin Sensor. *Nature* **2018**, *555* (7696), 351–354. <https://doi.org/10.1038/nature25781>.
- (19) Aslam, N.; Pfender, M.; Neumann, P.; Reuter, R.; Zappe, A.; De Oliveira, F. F.; Denisenko, A.; Sumiya, H.; Onoda, S.; Isoya, J.; et al. Nanoscale Nuclear Magnetic Resonance with Chemical Resolution. *Science* (80-.). **2017**, *357* (6346), 67–71. <https://doi.org/10.1126/science.aam8697>.
- (20) Jelezko, F.; Wrachtrup, J. Single Defect Centres in Diamond: A Review. *Phys.*

status solidi **2006**, *203* (13), 3207–3225. <https://doi.org/10.1002/pssa.200671403>.

- (21) Kolesov, R.; Xia, K.; Reuter, R.; Stöhr, R.; Zappe, A.; Meijer, J.; Hemmer, P. R.; Wrachtrup, J. Optical Detection of a Single Rare-Earth Ion in a Crystal. *Nat. Commun.* **2012**, *3* (1), 1–7. <https://doi.org/10.1038/ncomms2034>.
- (22) Wolfowicz, G.; Anderson, C. P.; Diler, B.; Poluektov, O. G.; Heremans, F. J.; Awschalom, D. D. Vanadium Spin Qubits as Telecom Quantum Emitters in Silicon Carbide. **2019**.
- (23) Dibos, A.; Raha, M.; Phenicie, C.; Thompson, J. Isolating and Enhancing the Emission of Single Erbium Ions Using a Silicon Nanophotonic Cavity. *Phys. Rev. Lett.* **2017**, *120* (24). <https://doi.org/10.1103/PhysRevLett.120.243601>.
- (24) Zhong, T.; Kindem, J. M.; Bartholomew, J. G.; Rochman, J.; Craiciu, I.; Verma, V.; Nam, S. W.; Marsili, F.; Shaw, M. D.; Beyer, A. D.; et al. Optically Addressing Single Rare-Earth Ions in a Nanophotonic Cavity. *Phys. Rev. Lett.* **2018**, *121* (18), 183603. <https://doi.org/10.1103/PhysRevLett.121.183603>.
- (25) Weber, J. R.; Koehl, W. F.; Varley, J. B.; Janotti, A.; Buckley, B. B.; Van De Walle, C. G.; Awschalom, D. D. Quantum Computing with Defects. *Proc. Natl. Acad. Sci. U. S. A.* **2010**, *107* (19), 8513–8518.
<https://doi.org/10.1073/pnas.1003052107>.
- (26) Markham, M. L.; Dodson, J. M.; Scarsbrook, G. A.; Twitchen, D. J.; Balasubramanian, G.; Jelezko, F.; Wrachtrup, J. CVD Diamond for Spintronics. *Diam. Relat. Mater.* **2011**, *20* (2), 134–139.
<https://doi.org/10.1016/j.diamond.2010.11.016>.
- (27) Balasubramanian, G.; Neumann, P.; Twitchen, D.; Markham, M.; Kolesov, R.; Mizuuchi, N.; Isoya, J.; Achard, J.; Beck, J.; Tissler, J.; et al. Ultralong Spin Coherence Time in Isotopically Engineered Diamond. *Nat. Mater.* **2009**, *8* (5), 383–387. <https://doi.org/10.1038/nmat2420>.
- (28) Tyryshkin, A. M.; Tojo, S.; Morton, J. J. L.; Riemann, H.; Abrosimov, N. V.; Becker, P.; Pohl, H. J.; Schenkel, T.; Thewalt, M. L. W.; Itoh, K. M.; et al. Electron Spin Coherence Exceeding Seconds in High-Purity Silicon. *Nat. Mater.* **2012**, *11* (2), 143–147. <https://doi.org/10.1038/nmat3182>.
- (29) Ong, S. P.; Cholia, S.; Jain, A.; Brafman, M.; Gunter, D.; Ceder, G.; Persson, K. A. The Materials Application Programming Interface (API): A Simple, Flexible and Efficient API for Materials Data Based on REpresentational State Transfer (REST) Principles. *Comput. Mater. Sci.* **2015**, *97*, 209–215.
<https://doi.org/10.1016/j.commatsci.2014.10.037>.
- (30) Jain, A.; Ong, S. P.; Hautier, G.; Chen, W.; Richards, W. D.; Dacek, S.; Cholia, S.; Gunter, D.; Skinner, D.; Ceder, G.; et al. Commentary: The Materials Project: A

Materials Genome Approach to Accelerating Materials Innovation. *APL Materials*. American Institute of Physics Inc. July 18, 2013, p 011002. <https://doi.org/10.1063/1.4812323>.

- (31) Kresse, G.; Furthmüller, J. Efficient Iterative Schemes for Ab Initio Total-Energy Calculations Using a Plane-Wave Basis Set. *Phys. Rev. B - Condens. Matter Mater. Phys.* **1996**, *54* (16), 11169–11186. <https://doi.org/10.1103/PhysRevB.54.11169>.
- (32) Wang, L.; Maxisch, T.; Ceder, G. Oxidation Energies of Transition Metal Oxides within the GGA+U Framework. *Phys. Rev. B - Condens. Matter Mater. Phys.* **2006**, *73* (19), 195107. <https://doi.org/10.1103/PhysRevB.73.195107>.
- (33) Choudhary, K.; Kalish, I.; Beams, R.; Tavazza, F. High-Throughput Identification and Characterization of Two-Dimensional Materials Using Density Functional Theory. *Sci. Rep.* **2017**, *7* (1), 1–16. <https://doi.org/10.1038/s41598-017-05402-0>.
- (34) Thonhauser, T.; Cooper, V. R.; Li, S.; Puzder, A.; Hyldgaard, P.; Langreth, D. C. Van Der Waals Density Functional: Self-Consistent Potential and the Nature of the van Der Waals Bond. *Phys. Rev. B - Condens. Matter Mater. Phys.* **2007**, *76* (12), 125112. <https://doi.org/10.1103/PhysRevB.76.125112>.
- (35) Klime, J.; Bowler, D. R.; Michaelides, A. Van Der Waals Density Functionals Applied to Solids. *Phys. Rev. B - Condens. Matter Mater. Phys.* **2011**, *83* (19), 195131. <https://doi.org/10.1103/PhysRevB.83.195131>.
- (36) Choudhary, K.; Zhang, Q.; Reid, A. C. E.; Chowdhury, S.; Van Nguyen, N.; Trautt, Z.; Newrock, M. W.; Congo, F. Y.; Tavazza, F. Computational Screening of High-Performance Optoelectronic Materials Using OptB88vdW and TB-MBJ Formalisms. *Sci. Data* **2018**, *5* (1), 1–12. <https://doi.org/10.1038/sdata.2018.82>.
- (37) Calderon, C. E.; Plata, J. J.; Toher, C.; Oses, C.; Levy, O.; Fornari, M.; Natan, A.; Mehl, M. J.; Hart, G.; Buongiorno Nardelli, M.; et al. The AFLOW Standard for High-Throughput Materials Science Calculations. *Comput. Mater. Sci.* **2015**, *108*, 233–238. <https://doi.org/10.1016/j.commatsci.2015.07.019>.
- (38) Curtarolo, S.; Setyawan, W.; Hart, G. L. W.; Jahnatek, M.; Chepulskii, R. V.; Taylor, R. H.; Wang, S.; Xue, J.; Yang, K.; Levy, O.; et al. AFLOW: An Automatic Framework for High-Throughput Materials Discovery. *Comput. Mater. Sci.* **2012**, *58*, 218–226. <https://doi.org/10.1016/j.commatsci.2012.02.005>.
- (39) Setyawan, W.; Curtarolo, S. High-Throughput Electronic Band Structure Calculations: Challenges and Tools. *Comput. Mater. Sci.* **2010**, *49* (2), 299–312. <https://doi.org/10.1016/j.commatsci.2010.05.010>.
- (40) Setyawan, W.; Gaume, R. M.; Lam, S.; Feigelson, R. S.; Curtarolo, S. High-Throughput Combinatorial Database of Electronic Band Structures for Inorganic Scintillator Materials. *ACS Comb. Sci.* **2011**, *13* (4), 382–390.

<https://doi.org/10.1021/co200012w>.

- (41) Isayev, O.; Oses, C.; Toher, C.; Gossett, E.; Curtarolo, S.; Tropsha, A. Universal Fragment Descriptors for Predicting Properties of Inorganic Crystals. *Nature Communications*. Nature Publishing Group June 5, 2017, pp 1–12. <https://doi.org/10.1038/ncomms15679>.
- (42) Perdew, J. P. Density Functional Theory and the Band Gap Problem. *Int. J. Quantum Chem.* **2009**, *28* (S19), 497–523. <https://doi.org/10.1002/qua.560280846>.
- (43) Wort, C. J. H.; Balmer, R. S. Diamond as an Electronic Material. *Materials Today*. Elsevier January 1, 2008, pp 22–28. [https://doi.org/10.1016/S1369-7021\(07\)70349-8](https://doi.org/10.1016/S1369-7021(07)70349-8).
- (44) Rabenau, T.; Simon, A.; Kremer, R. K.; Sohmen, E. The Energy Gaps of Fullerene C₆₀ and C₇₀ Determined from the Temperature Dependent Microwave Conductivity. *Zeitschrift für Phys. B Condens. Matter* **1993**, *90* (1), 69–72. <https://doi.org/10.1007/BF01321034>.
- (45) Abass, A. K.; Ahmad, N. H. Indirect Band Gap Investigation of Orthorhombic Single Crystals of Sulfur. *J. Phys. Chem. Solids* **1986**, *47* (2), 143–145. [https://doi.org/10.1016/0022-3697\(86\)90123-X](https://doi.org/10.1016/0022-3697(86)90123-X).
- (46) Nagata, K.; Miyamoto, Y.; Nishimura, H.; Suzuki, H.; Yamasaki, S. Photoconductivity and Photoacoustic Spectra of Trigonal, Rhombohedral, Orthorhombic, and α -, β -, and γ -Monoclinic Selenium. *Jpn. J. Appl. Phys.* **1985**, *24* (11), L858–L860. <https://doi.org/10.1143/JJAP.24.L858>.
- (47) Macfarlane, G. G.; McLean, T. P.; Quarrington, J. E.; Roberts, V. Fine Structure in the Absorption-Edge Spectrum of Si. *Phys. Rev.* **1958**, *111* (5), 1245–1254. <https://doi.org/10.1103/PhysRev.111.1245>.
- (48) Kim, D. Y.; Stefanoski, S.; Kurakevych, O. O.; Strobel, T. A. Synthesis of an Open-Framework Allotrope of Silicon. *Nat. Mater.* **2015**, *14* (2), 169–173. <https://doi.org/10.1038/nmat4140>.
- (49) Gryko, J.; McMillan, P. F.; Marzke, R. F.; Ramachandran, G. K.; Patton, D.; Deb, S. K.; Sankey, O. F. *Low-Density Framework Form of Crystalline Silicon with a Wide Optical Band Gap*; 2000; Vol. 62. <https://doi.org/10.1103/PhysRevB.62.R7707>.
- (50) Feng, J.; Xiao, B.; Chen, J. Crystal Structures and Electronic Properties of BaC₂ Isomers by Theoretical Study Based on DFT. *Sci. China, Ser. B Chem.* **2008**, *51* (6), 545–550. <https://doi.org/10.1007/s11426-008-0034-3>.
- (51) Saum, G. A.; Hensley, E. B. Fundamental Optical Absorption in the IIA-VIB Compounds. *Phys. Rev.* **1959**, *113* (1958), 1019–1022.

- (52) Nakamura, T.; Suemasu, T.; Takakura, K. I.; Hasegawa, F.; Wakahara, A.; Imai, M. Investigation of the Energy Band Structure of Orthorhombic BaSi₂ by Optical and Electrical Measurements and Theoretical Calculations. *Appl. Phys. Lett.* **2002**, *81* (6), 1032–1034. <https://doi.org/10.1063/1.1498865>.
- (53) Neeley, V. I.; Kemp, J. C. Optical Absorption in CaO Single Crystals. *J. Phys. Chem. Solids* **1963**, *24* (11), 1301–1304. [https://doi.org/10.1016/0022-3697\(63\)90174-4](https://doi.org/10.1016/0022-3697(63)90174-4).
- (54) Nelson, J. R.; Needs, R. J.; Pickard, C. J. Calcium Peroxide from Ambient to High Pressures. *Phys. Chem. Chem. Phys.* **2015**, *17* (10), 6889–6895. <https://doi.org/10.1039/c4cp05644b>.
- (55) Pajasová, L. Optical Properties of GeO₂ in the Ultraviolet Region. *Czechoslov. J. Phys.* **1969**, *19* (10), 1265–1270. <https://doi.org/10.1007/BF01690313>.
- (56) D'Amboise, M.; Handfield, G.; Bourgon, M. Apparent Activation Energies for Electrical Conduction of Solid and Liquid Germanium(II) Sulfide. *Can. J. Chem.* **1968**, *46* (22), 3545–3550. <https://doi.org/10.1139/v68-587>.
- (57) Lukeš, F. Optical and Photoelectric Properties of GeSe in the Energy Range 0·5–1·5 EV. *Czechoslov. J. Phys.* **1968**, *18* (6), 784–794. <https://doi.org/10.1007/BF01696140>.
- (58) Gavaleshko, N. P.; Kurisk, M. V.; Savchuk, A. I. ABSORPTION EDGE OF GESE2. *Sov. Phys. Semicond.* **1968**, *1*, 920.
- (59) Afanas'ev, V. V.; Stesmans, A.; Chen, F.; Shi, X.; Campbell, S. A. Internal Photoemission of Electrons and Holes from (100)Si into HfO₂. *Appl. Phys. Lett.* **2002**, *81* (6), 1053–1055. <https://doi.org/10.1063/1.1495088>.
- (60) Kreis, C.; Werth, S.; Adelung, R.; Kipp, L.; Skibowski, M.; Krasovskii, E. E.; Schattke, W. Valence and Conduction Band States of HfS₂: From Bulk to a Single Layer. *Phys. Rev. B - Condens. Matter Mater. Phys.* **2003**, *68* (23), 235331. <https://doi.org/10.1103/PhysRevB.68.235331>.
- (61) Srivastava, S. K.; Avasthi, B. N. Preparation, Structure and Properties of Transition Metal Trichalcogenides. *Journal of Materials Science*. Kluwer Academic Publishers January 1, 1992, pp 3693–3705. <https://doi.org/10.1007/BF00545445>.
- (62) Wang, D.; Yan, Y.; Zhou, D.; Liu, Y. Evolution of Crystal and Electronic Structures of Magnesium Dicarbide at High Pressure. *Sci. Rep.* **2015**, *5* (1), 1–8. <https://doi.org/10.1038/srep17815>.
- (63) Strobel, T. A.; Kurakevych, O. O.; Kim, D. Y.; Le Godec, Y.; Crichton, W.; Guignard, J.; Guignot, N.; Cody, G. D.; Oganov, A. R. Synthesis of β -Mg₂C₃: A Monoclinic High-Pressure Polymorph of Magnesium Sesquicarbide. *Inorg. Chem.* **2014**, *53* (13), 7020–7027. <https://doi.org/10.1021/ic500960d>.

- (64) Bhandari, U.; Bamba, C. O.; Malozovsky, Y.; Franklin, L. S.; Bagayoko, D. Predictions of Electronic, Transport, and Structural Properties of Magnesium Sulfide (MgS) in the Rocksalt Structure. *J. Mod. Phys.* **2018**, *09* (09), 1773–1784. <https://doi.org/10.4236/jmp.2018.99111>.
- (65) Kolb, B.; Kolpak, A. M. Ultrafast Band-Gap Oscillations in Iron Pyrite. *Phys. Rev. B - Condens. Matter Mater. Phys.* **2013**, *88* (23), 235208. <https://doi.org/10.1103/PhysRevB.88.235208>.
- (66) Bouzidi, A.; Benramdane, N.; Tabet-Derraz, H.; Mathieu, C.; Khelifa, B.; Desfeux, R. Effect of Substrate Temperature on the Structural and Optical Properties of MoO₃ Thin Films Prepared by Spray Pyrolysis Technique. *Mater. Sci. Eng. B Solid-State Mater. Adv. Technol.* **2003**, *97* (1), 5–8. [https://doi.org/10.1016/S0921-5107\(02\)00385-9](https://doi.org/10.1016/S0921-5107(02)00385-9).
- (67) Lu, C. P.; Li, G.; Mao, J.; Wang, L. M.; Andrei, E. Y. Bandgap, Mid-Gap States, and Gating Effects in MoS₂. *Nano Lett.* **2014**, *14* (8), 4628–4633. <https://doi.org/10.1021/nl501659n>.
- (68) Kohara, N.; Nishiwaki, S.; Hashimoto, Y.; Negami, T.; Wada, T. Electrical Properties of the Cu(In,Ga)Se₂/MoSe₂/Mo Structure. *Sol. Energy Mater. Sol. Cells* **2001**, *67* (1–4), 209–215. [https://doi.org/10.1016/S0927-0248\(00\)00283-X](https://doi.org/10.1016/S0927-0248(00)00283-X).
- (69) Mondal, P. S.; Okazaki, R.; Taniguchi, H.; Terasaki, I. Photo-Seebeck Effect in Tetragonal PbO Single Crystals. *J. Appl. Phys.* **2013**, *114* (17), 173710. <https://doi.org/10.1063/1.4829460>.
- (70) Keester, K. L.; White, W. B. Electronic Spectra of the Oxides of Lead and of Some Ternary Lead Oxide Compounds. *Mater. Res. Bull.* **1969**, *4* (10), 757–764. [https://doi.org/10.1016/0025-5408\(69\)90066-X](https://doi.org/10.1016/0025-5408(69)90066-X).
- (71) Huang, Y. S.; Lin, S. S. Growth and Characterization of RuS₂ Single Crystals. *Mater. Res. Bull.* **1988**, *23* (2), 277–285. [https://doi.org/10.1016/0025-5408\(88\)90105-5](https://doi.org/10.1016/0025-5408(88)90105-5).
- (72) Persson, C.; Lindefelt, U. Detailed Band Structure for 3C-, 2H-, 4H-, 6H-SiC, and Si around the Fundamental Band Gap. *Phys. Rev. B - Condens. Matter Mater. Phys.* **1996**, *54* (15), 10257–10260. <https://doi.org/10.1103/PhysRevB.54.10257>.
- (73) Garvie, L. A. J.; Rez, P.; Alvarez, J. R.; Buseck, P. R. Interband Transitions of Crystalline and Amorphous SiO₂: An Electron Energy-Loss Spectroscopy (EELS) Study of the Low-Loss Region. *Solid State Commun.* **1998**, *106* (5), 303–307. [https://doi.org/10.1016/S0038-1098\(98\)00021-0](https://doi.org/10.1016/S0038-1098(98)00021-0).
- (74) Bletskan, D. I.; Vakulchak, V. V.; Glukhov, K. E. Electronic Structure of Low-Pressure and High-Pressure Phases of Silicon Disulfide. *Appl. Phys. A Mater. Sci. Process.* **2014**, *117* (3), 1499–1514. <https://doi.org/10.1007/s00339-014-8584-z>.

- (75) Sensato, F. R.; Custódio, R.; Calatayud, M.; Beltrán, A.; Andrés, J.; Sambrano, J. R.; Longo, E. Periodic Study on the Structural and Electronic Properties of Bulk, Oxidized and Reduced SnO₂(1 1 0) Surfaces and the Interaction with O₂. *Surf. Sci.* **2002**, *511* (1–3), 408–420. [https://doi.org/10.1016/S0039-6028\(02\)01542-X](https://doi.org/10.1016/S0039-6028(02)01542-X).
- (76) Burton, L. A.; Colombara, D.; Abellon, R. D.; Grozema, F. C.; Peter, L. M.; Savenije, T. J.; Dennler, G.; Walsh, A. Synthesis, Characterization, and Electronic Structure of Single-Crystal SnS, Sn₂S₃, and SnS₂. *Chem. Mater.* **2013**, *25* (24), 4908–4916. <https://doi.org/10.1021/cm403046m>.
- (77) Shameem Banu, I. B.; Rajagopalan, M.; Palanivel, B.; Kalpana, G.; Shenbagaraman, P. Structural and Electronic Properties of SrS, SrSe, and SrTe under Pressure. *J. Low Temp. Phys.* **1998**, *112* (3–4), 211–226. <https://doi.org/10.1023/A:1022685715644>.
- (78) Moufok, S.; Kadi, L.; Amrani, B.; Khodja, K. D. Electronic Structure and Optical Properties of TeO₂ Polymorphs. *Results Phys.* **2019**, *13*, 102315. <https://doi.org/10.1016/j.rinp.2019.102315>.
- (79) Roginskii, E. M.; Smirnov, M. B.; Kuznetsov, V. G.; Noguera, O.; Cornette, J.; Masson, O.; Thomas, P. A Computational Study of the Electronic Structure and Optical Properties of the Complex TeO₂/TeO₃ Oxides as Advanced Materials for Nonlinear Optics. *Mater. Res. Express* **2019**, *6*, 125903. <https://doi.org/10.1088/2053-1591/ab55a3>.
- (80) Roginskii, E. M.; Kuznetsov, V. G.; Smirnov, M. B.; Noguera, O.; Duclère, J. R.; Colas, M.; Masson, O.; Thomas, P. Comparative Analysis of the Electronic Structure and Nonlinear Optical Susceptibility of α -TeO₂ and β -TeO₃ Crystals. *J. Phys. Chem. C* **2017**, *121* (22), 12365–12374. <https://doi.org/10.1021/acs.jpcc.7b01819>.
- (81) Tang, H.; Lévy, F.; Berger, H.; Schmid, P. E. Urbach Tail of Anatase TiO₂. *Phys. Rev. B* **1995**, *52* (11), 7771–7774. <https://doi.org/10.1103/PhysRevB.52.7771>.
- (82) Pascual, J.; Camassel, J.; Mathieu, H. Fine Structure in the Intrinsic Absorption Edge of TiO₂. *Phys. Rev. B* **1978**, *18* (10), 5606–5614. <https://doi.org/10.1103/PhysRevB.18.5606>.
- (83) Wang, F.; Di Valentin, C.; Pacchioni, G. Electronic and Structural Properties of WO₃: A Systematic Hybrid DFT Study. *J. Phys. Chem. C* **2011**, *115* (16), 8345–8353. <https://doi.org/10.1021/jp201057m>.
- (84) Upadhyayula, L. C.; Loferski, J. J.; Wold, A.; Giri, W.; Kershaw, R. Semiconducting Properties of Single Crystals of N- and P-Type Tungsten Diselenide (WSe₂). *J. Appl. Phys.* **1968**, *39* (10), 4736–4740. <https://doi.org/10.1063/1.1655829>.

- (85) Wang, J.; Wang, Z.; Huang, B.; Ma, Y.; Liu, Y.; Qin, X.; Zhang, X.; Dai, Y. Oxygen Vacancy Induced Band-Gap Narrowing and Enhanced Visible Light Photocatalytic Activity of ZnO. *ACS Appl. Mater. Interfaces* **2012**, *4* (8), 4024–4030. <https://doi.org/10.1021/am300835p>.
- (86) Sooklal, K.; Cullum, B. S.; Angel, S. M.; Murphy, C. J. Photophysical Properties of ZnS Nanoclusters with Spatially Localized Mn²⁺. *J. Phys. Chem.* **1996**, *100* (11), 4551–4555. <https://doi.org/10.1021/jp952377a>.
- (87) Liu, T.-L.; Zhang, J.-M.; Bullett, D. W. *Electronic Structure of 3d Pyrite-and Marcasite-Type Sulphides*; 1982; Vol. 15.
- (88) Chadi, D. J. Doping in ZnSe, ZnTe, MgSe, and MgTe Wide-Band-Gap Semiconductors. *Phys. Rev. Lett.* **1994**, *72* (4), 534–537. <https://doi.org/10.1103/PhysRevLett.72.534>.
- (89) Jiang, H.; Gomez-Abal, R. I.; Rinke, P.; Scheffler, M. Electronic Band Structure of Zirconia and Hafnia Polymorphs from the GW Perspective. <https://doi.org/10.1103/PhysRevB.81.085119>.
- (90) Mañas-Valero, S.; García-López, V.; Cantarero, A.; Galbiati, M. Raman Spectra of ZrS₂ and ZrSe₂ from Bulk to Atomically Thin Layers. *Appl. Sci.* **2016**, *6* (9), 264. <https://doi.org/10.3390/app6090264>.
- (91) Kurita, S.; Staehli, J. L.; Guzzi, M.; Lévy, F. Optical Properties of ZrS₃ and ZrSe₃. *Phys. B+C* **1981**, *105* (1–3), 169–173. [https://doi.org/10.1016/0378-4363\(81\)90239-4](https://doi.org/10.1016/0378-4363(81)90239-4).
- (92) Wu, K.; Pan, S.; Yang, Z. Ba₂GeS₄ and Mg₂SnS₄: Synthesis, Structures, Optical Properties and Electronic Structures. *RSC Adv.* **2015**, *5* (42), 33646–33652. <https://doi.org/10.1039/c5ra00264h>.
- (93) Pan, M. Y.; Xia, S. Q.; Liu, X. C.; Tao, X. T. Ba₃GeS₅ and Ba₃InS₄Cl: Interesting Size Effects Originated from the Tetrahedral Anions. *J. Solid State Chem.* **2014**, *219*, 74–79. <https://doi.org/10.1016/j.jssc.2014.07.009>.
- (94) Kormath Madam Raghupathy, R.; Wiebeler, H.; Kühne, T. D.; Felser, C.; Mirhosseini, H. Database Screening of Ternary Chalcogenides for P-Type Transparent Conductors. *Chem. Mater.* **2018**, *30* (19), 6794–6800. <https://doi.org/10.1021/acs.chemmater.8b02719>.
- (95) Johrendt, D.; Tampier, M. Strontium Selenogermanate(III) and Barium Selenogermanate(II,IV): Synthesis, Crystal Structures, and Chemical Bonding. *Chem. – A Eur. J.* **2000**, *6* (6), 994–998. [https://doi.org/10.1002/\(SICI\)1521-3765\(20000317\)6:6<994::AID-CHEM994>3.0.CO;2-H](https://doi.org/10.1002/(SICI)1521-3765(20000317)6:6<994::AID-CHEM994>3.0.CO;2-H).
- (96) Hanzawa, K.; Iimura, S.; Hiramatsu, H.; Hosono, H. Material Design of Green-Light-Emitting Semiconductors: Perovskite-Type Sulfide SrHfS₃. *J. Am. Chem.*

Soc. **2019**, *141* (13), 5343–5349. <https://doi.org/10.1021/jacs.8b13622>.

- (97) Li, W.; Niu, S.; Zhao, B.; Haiges, R.; Zhang, Z.; Ravichandran, J.; Janotti, A. Band Gap Evolution in Ruddlesden-Popper Phases. *Phys. Rev. Mater.* **2019**, *3*, 101601. <https://doi.org/10.1103/PhysRevMaterials.3.101601>.
- (98) Fu, W. T.; Van Ruitenbeek, J. M.; Xu, Q.; Van Ruitenbeek, J. M.; De Jongh, L. J. Physical Properties of the Monolayer Compounds Ba₂Pb_{1-x}BixO₄ Graphene Single-Molecule Nanopore Sensors for Future Real-Time Sequencing of DNA View Project Two Dimensional Materials View Project PHYSICAL PROPERTIES OF THE MONOLAYER COMPOUNDS Ba₂Pb_{1-x}BixO₄. *PhysicaC* **1990**, *167*, 271–277. [https://doi.org/10.1016/0921-4534\(90\)90341-B](https://doi.org/10.1016/0921-4534(90)90341-B).
- (99) Kim, H. J.; Kim, U.; Kim, H. M.; Kim, T. H.; Mun, H. S.; Jeon, B. G.; Hong, K. T.; Lee, W. J.; Ju, C.; Kimy, K. H.; et al. High Mobility in a Stable Transparent Perovskite Oxide. *Appl. Phys. Express* **2012**, *5* (6), 061102. <https://doi.org/10.1143/APEX.5.061102>.
- (100) Omeiri, S.; Rekhila, G.; Trari, M.; Bessekhouad, Y. Physical and Photoelectrochemical Characterizations of Ba₂SnO_{4-δ} Elaborated by Chemical Route. *J. Solid State Electrochem.* **2015**, *19* (6), 1651–1658. <https://doi.org/10.1007/s10008-015-2786-y>.
- (101) Ha, V. A.; Yu, G.; Ricci, F.; Dahliah, D.; Van Setten, M. J.; Giantomassi, M.; Rignanese, G. M.; Hautier, G. Computationally Driven High-Throughput Identification of CaTe and Li₃Sb as Promising Candidates for High-Mobility p - Type Transparent Conducting Materials. *Phys. Rev. Mater.* **2019**, *3* (3), 034601. <https://doi.org/10.1103/PhysRevMaterials.3.034601>.
- (102) Luo, Z. Z.; Lin, C. S.; Cheng, W. D.; Zhang, H.; Zhang, W. L.; He, Z. Z. Syntheses, Characterization, and Optical Properties of Ternary Ba-Sn-S System Compounds: Acentric Ba₇Sn₅S₁₅, Centric BaSn₂S₅, and Centric Ba₆Sn₇S₂₀. *Inorg. Chem.* **2013**, *52* (1), 273–279. <https://doi.org/10.1021/ic301804n>.
- (103) Wu, K.; Su, X.; Yang, Z.; Pan, S. An Investigation of New Infrared Nonlinear Optical Material: BaCdSnSe₄, and Three New Related Centrosymmetric Compounds: Ba₂SnSe₄, Mg₂GeSe₄, and Ba₂Ge₂S₆. *Dalt. Trans.* **2015**, *44* (46), 19856–19864. <https://doi.org/10.1039/c5dt03215f>.
- (104) Assoud, A.; Soheilnia, N.; Kleinke, H. The New Semiconducting Polychalcogenide Ba₂SnSe₅ Exhibiting Se₂₋₃ Units and Distorted SnSe₆ Octahedra. *J. Solid State Chem.* **2005**, *178* (4), 1087–1093. <https://doi.org/10.1016/j.jssc.2005.01.011>.
- (105) Feng, K.; Jiang, X.; Kang, L.; Yin, W.; Hao, W.; Lin, Z.; Yao, J.; Wu, Y.; Chen, C. Ba₆Sn₆Se₁₃: A New Mixed Valence Selenostannate with NLO Property. *Dalt. Trans.* **2013**, *42* (37), 13635–13641. <https://doi.org/10.1039/c3dt51317c>.

- (106) Assoud, A.; Kleinke, H. Unique Barium Selenostannate-Selenide: Ba₇Sn₃Se₁₃ (and Its Variants Ba₇Sn₃Se₁₃-ΔTeδ) with SnSe₄ Tetrahedra and Isolated Se Anions. *Chem. Mater.* **2005**, *17* (17), 4509–4513. <https://doi.org/10.1021/cm050787y>.
- (107) Mishra, K. K.; Achary, S. N.; Chandra, S.; Ravindran, T. R.; Sinha, A. K.; Singh, M. N.; Tyagi, A. K. Structural and Thermal Properties of BaTe₂O₆: Combined Variable-Temperature Synchrotron X-Ray Diffraction, Raman Spectroscopy, and Ab Initio Calculations. *Inorg. Chem.* **2016**, *55* (17), 8994–9005. <https://doi.org/10.1021/acs.inorgchem.6b01476>.
- (108) Sun, J.; Shi, H.; Du, M. H.; Siegrist, T.; Singh, D. J. Ba₂TeO as an Optoelectronic Material: First-Principles Study. *J. Appl. Phys.* **2015**, *117* (19), 195705. <https://doi.org/10.1063/1.4921585>.
- (109) Lacomba-Perales, R.; Ruiz-Fuertes, J.; Errandonea, D.; Martínez-García, D.; Segura, A. Optical Absorption of Divalent Metal Tungstates: Correlation between the Band-Gap Energy and the Cation Ionic Radius. *EPL (Europhysics Lett.)* **2008**, *83* (3), 37002. <https://doi.org/10.1209/0295-5075/83/37002>.
- (110) Wang, Y. X.; Hu, C. E.; Chen, Y. M.; Cheng, Y.; Ji, G. F. First-Principles Study of the Structural, Optical, Dynamical and Thermodynamic Properties of BaZnO₂ Under Pressure. *Int. J. Thermophys.* **2016**, *37* (11), 1–18. <https://doi.org/10.1007/s10765-016-2115-4>.
- (111) Lin, Y. F.; Chang, Y. H.; Chang, Y. S.; Tsai, B. S.; Li, Y. C. Photoluminescent Properties of Ba₂ZnS₃:Mn Phosphors. *J. Alloys Compd.* **2006**, *421* (1–2), 268–272. <https://doi.org/10.1016/j.jallcom.2005.11.038>.
- (112) Zhou, M.; Xiao, K.; Jiang, X.; Huang, H.; Lin, Z.; Yao, J.; Wu, Y. Visible-Light-Responsive Chalcogenide Photocatalyst Ba₂ZnSe₃: Crystal and Electronic Structure, Thermal, Optical, and Photocatalytic Activity. *Inorg. Chem.* **2016**, *55* (24), 12783–12790. <https://doi.org/10.1021/acs.inorgchem.6b02072>.
- (113) Prakash, J.; Mesbah, A.; Beard, J.; Rocca, D.; Lebègue, S.; Malliakas, C. D.; Ibers, J. A. Two New Ternary Chalcogenides Ba₂ZnQ₃ (Q = Se, Te) with Chains of ZnQ₄ Tetrahedra: Syntheses, Crystal Structure, and Optical and Electronic Properties. *Zeitschrift fur Naturforsch. - Sect. B J. Chem. Sci.* **2016**, *71* (5), 425–429. <https://doi.org/10.1515/znb-2015-0226>.
- (114) Li, L.; Yu, W.; Long, Y.; Jin, C. First-Principles Calculations on the Pressure Induced Zircon-Type to Scheelite-Type Phase Transition of CaCrO₄. *Solid State Commun.* **2006**, *137* (7), 358–361. <https://doi.org/10.1016/j.ssc.2005.12.021>.
- (115) Chen, J.; Chai, F.; Yin, T.; Zhang, H.-Y.; Fu, S.-L. Photoluminescence of Eu(3+)-Doped Ca₂PbO₄ with One-Dimensional Structure. *Chinese J. Inorg. Chem.* **2007**, *23* (10), 1801–1804.

- (116) Henriques, J. M.; Caetano, E. W. S.; Freire, V. N.; Da Costa, J. A. P.; Albuquerque, E. L. Structural, Electronic, and Optical Absorption Properties of Orthorhombic CaSnO₃ through Ab Initio Calculations. *J. Phys. Condens. Matter* **2007**, *19* (10). <https://doi.org/10.1088/0953-8984/19/10/106214>.
- (117) Mizoguchi, H.; Woodward, P. M. Electronic Structure Studies of Main Group Oxides Possessing Edge-Sharing Octahedra: Implications for the Design of Transparent Conducting Oxides. *Chem. Mater.* **2004**, *16* (25), 5233–5248. <https://doi.org/10.1021/cm049249w>.
- (118) Perera, S.; Hui, H.; Zhao, C.; Xue, H.; Sun, F.; Deng, C.; Gross, N.; Milleville, C.; Xu, X.; Watson, D. F.; et al. Chalcogenide Perovskites - an Emerging Class of Ionic Semiconductors. *Nano Energy* **2016**, *22*, 129–135. <https://doi.org/10.1016/j.nanoen.2016.02.020>.
- (119) Bletskan, D. I.; Kabacij, V. N.; Studenyak, I. P.; Frolova, V. V. Edge Absorption Spectra of Crystalline and Glassy PbGeS₃. *Opt. Spectrosc. (English Transl. Opt. i Spektrosk.)* **2007**, *103* (5), 772–776. <https://doi.org/10.1134/S0030400X0711015X>.
- (120) Hautier, G.; Miglio, A.; Ceder, G.; Rignanese, G. M.; Gonze, X. Identification and Design Principles of Low Hole Effective Mass P-Type Transparent Conducting Oxides. *Nat. Commun.* **2013**, *4* (1), 1–7. <https://doi.org/10.1038/ncomms3292>.
- (121) Hersh, P. A. Wide Band Gap Semiconductors and Insulators: Synthesis, Processing and Characterization, Oregon State University, 2007.
- (122) Popovic, Z. Optical Phonons in SnGeS₃ Raman Scattering and Photoluminescence Study of Laser Modified Nanocrystalline ZnO Thin Films Suitable for Sensor Applications View Project Nanostructured Multifunctional Materials and Nanocomposites (III45018)-Numerical Models View Project. <https://doi.org/10.1103/PhysRevB.32.2382>.
- (123) Noor, N. A.; Mahmood, Q.; Rashid, M.; Ul Haq, B.; Laref, A. The Pressure-Induced Mechanical and Optoelectronic Behavior of Cubic Perovskite PbSnO₃ via Ab-Initio Investigations. *Ceram. Int.* **2018**, *44* (12), 13750–13756. <https://doi.org/10.1016/j.ceramint.2018.04.217>.
- (124) Hadjarab, B.; Saadi, S.; Bouguelia, A.; Trari, M. Physical Properties and Photoelectrochemical Characterization of SrPbO₃. *Phys. status solidi* **2007**, *204* (7), 2369–2380. <https://doi.org/10.1002/pssa.200622296>.
- (125) Bellal, B.; Hadjarab, B.; Bouguelia, A.; Trari, M. Visible Light Photocatalytic Reduction of Water Using SrSnO₃ Sensitized by CuFeO₂. *Theor. Exp. Chem.* **2009**, *45* (3), 172–179. <https://doi.org/10.1007/s11237-009-9080-y>.
- (126) Niu, S.; Huyan, H.; Liu, Y.; Yeung, M.; Ye, K.; Blankemeier, L.; Orvis, T.; Sarkar, D.; Singh, D. J.; Kapadia, R.; et al. Bandgap Control via Structural and Chemical

- Tuning of Transition Metal Perovskite Chalcogenides. *Adv. Mater.* **2017**, *29* (9), 1604733. <https://doi.org/10.1002/adma.201604733>.
- (127) Gegner, J.; Gama, M.; Ackebauer, S. V.; Hollmann, N.; Hu, Z.; Hsieh, H. H.; Lin, H. J.; Chen, C. T.; Ormeci, A.; Leithe-Jasper, A.; et al. Insulator-Metal Transition in TiGePt: A Combined Photoelectron Spectroscopy, x-Ray Absorption Spectroscopy, and Band Structure Study. *Phys. Rev. B - Condens. Matter Mater. Phys.* **2012**, *85* (23), 235106. <https://doi.org/10.1103/PhysRevB.85.235106>.
- (128) Boltersdorf, J.; Sullivan, I.; Shelton, T. L.; Wu, Z.; Gray, M.; Zoellner, B.; Osterloh, F. E.; Maggard, P. A. Flux Synthesis, Optical and Photocatalytic Properties of n-Type Sn₂TiO₄: Hydrogen and Oxygen Evolution under Visible Light. *Chem. Mater.* **2016**, *28* (24), 8876–8889. <https://doi.org/10.1021/acs.chemmater.6b02003>.
- (129) Shannon, R. D.; Fischer, R. X.; Medenbach, O.; Bousquet, E.; Ghosez, P. Correlation between Optical Constants and Crystal Chemical Parameters of ZrW₂O₈. *J. Solid State Chem.* **2009**, *182* (10), 2762–2768. <https://doi.org/10.1016/j.jssc.2009.07.035>.
- (130) Assoud, A.; Soheilnia, N.; Kleinke, H. From Yellow to Black: New Semiconducting Ba Chalcogeno-Germanates. *Zeitschrift fur Naturforsch. - Sect. B J. Chem. Sci.* **2004**, *59* (9), 975–979. <https://doi.org/10.1515/znb-2004-0905>.
- (131) Zhang, S. Y.; Hu, C. L.; Mao, J. G. New Mixed Metal Selenites and Tellurites Containing Pd²⁺ Ions in a Square Planar Geometry. *Dalt. Trans.* **2012**, *41* (7), 2011–2017. <https://doi.org/10.1039/c1dt11836f>.
- (132) Broadley, S.; Gál, Z. A.; Corà, F.; Smura, C. F.; Clarke, S. J. Vertex-Linked ZnO₂S₂ Tetrahedra in the Oxysulfide BaZnOS: A New Coordination Environment for Zinc in a Condensed Solid. *Inorg. Chem.* **2005**, *44* (24), 9092–9096. <https://doi.org/10.1021/ic051240o>.
- (133) Aoba, T.; Tiittanen, T.; Suematsu, H.; Karppinen, M. Pressure-Induced Phase Transitions of Hexagonal Perovskite-like Oxides. *J. Solid State Chem.* **2016**, *233*, 492–496. <https://doi.org/10.1016/j.jssc.2015.11.028>.
- (134) Mehmood, S.; Ali, Z.; Hashmi, Z.; Khan, S. Structural, Optoelectronic and Elastic Properties of Quaternary Perovskites CaPd₃B₄O₁₂ (B = Ti, V). *Int. J. Mod. Phys. B* **2019**, *33* (19). <https://doi.org/10.1142/S0217979219502126>.
- (135) Zhang, S. Y.; Hu, C. L.; Li, P. X.; Jiang, H. L.; Mao, J. G. Syntheses, Crystal Structures and Properties of New Lead(Ii) or Bismuth(Iii) Selenites and Tellurite. *Dalt. Trans.* **2012**, *41* (31), 9532–9542. <https://doi.org/10.1039/c2dt30560g>.